Preliminary Design of Expendable and Reusable Mixed-Staged Launch Vehicles

Pawel Goldyn,* Ansgar Marwege,† Johannes Riehmer,‡ Josef Klevanski,§ and Ali Gülhan¶
German Aerospace Center (DLR e.V.), 51147 Cologne, Germany

One of the very first tasks in launch vehicle design is the preliminary sizing. It is necessary for further design choices, but it should deliver a precise estimate of the launch vehicle's mass and geometry as possible. Orbital launch vehicles can be either expendable or partially/fully reusable and can assume various stage configurations. Finding an optimal solution under practical constraints is a challenging task, which gives a wide design space for potential future launch vehicles. Hence, a generalized mathematical model of a launch vehicle design has been developed and implemented as a versatile and easily modifiable programming tool for fast and parametric system characterization and optimization. The model uses several basic parameters useful in describing launch vehicles and introduces some new parameters to account for reusability. Analytical and semi-empirical correlations are used to determine the overall system and mission performance of a launch vehicle for a given reference mission, including mass and geometry, and calculate the optimal launcher staging. The implementation of the model also allows coupling with other tools, which forms a design chain with respect to aerodynamics and trajectory simulation. With this design chain, several launch vehicles have been modeled and validated, proving the applicability of the method.

Nomenclature

a	=	orbit semimajor axis, m
e	=	orbit eccentricity
g_0	=	standard gravity, m/s²
h	=	height, orbit perigee altitude, m
i	=	orbit inclination, °
m	=	mass, stage net mass, kg
I_{sp}	=	specific impulse, s
K	=	ratio of the core to booster ascent propellant
T	=	thrust, N
t_B	=	burn time, s
γ	=	flight path angle, °
Δv	=	delta-v, m/s
ε	=	propellant-based structural index
ζ	=	stage throttling
Θ	=	thrust-to-weight ratio
λ	=	fraction of the core ascent propellant used until booster detachment
μ	=	mass ratio
ξ	=	reusability index
σ	=	mass-based structural index
φ_{LS}	=	launch site latitude
χ_v	=	design delta-v margin
ψ	=	dead propellant fraction

Subscripts

b	=	booster
c	=	core
exh	=	exhaust
k	=	kth stage
PL	=	payload
p	=	propellant
SL	=	sea level
s	=	structure
vac	=	vacuum
0	=	gross (mass)
1′	=	lower virtual stage
1″	=	upper virtual stage

Superscripts

A	=	ascent
D	=	descent
d	=	dry (structural index)
R	=	residual and reserve
w	=	wet (structural index)

I. Introduction

AT THE early development stage of a staged orbital launch vehicle (LV) design project, a tool for preliminary assessment of its mass, geometry, center of gravity (CoG), and moment of inertia (MoI), as well as a rudimentary visualization, is needed. This process is referred to as preliminary launcher design. In recent years, there has been an increase in interest in reusable LVs, but expendable ones still remain a sizable portion of the industry. Therefore, such a tool should account for both possibilities. LVs can assume various configurations (serial, parallel, or mixed-staged) and be composed of various components, so the tool should be able to calculate an arbitrary design with little to no workarounds. However, LV technologies quickly evolve, which makes it impossible to foresee all the possible design combinations, and hence a truly versatile tool should also be easily modifiable and expandable.

Several approaches to the topic of preliminary LV design have been undertaken so far. Contant [1] applied the multidisciplinary approach with the financial aspect of a project, focusing on small reusable LVs. Jentzsch [2] employed a genetic algorithm to optimize several input parameters of an LV, mainly relevant to propulsion, for the lowest gross liftoff weight (GLOW) and structural mass. Sippel [3] developed a tool optimizing an LV in a loop with trajectory; this tool has recently been used for a comparative analysis of reusable LVs by Wilken and Stappert [4]. Castellini [5] described the optimization of expendable LVs with extensive analysis of propulsion, geometry,

aerodynamics, trajectory, mass, structure, costs, and risks. Edberg and Costa [6] published a straightforward algorithm for preliminary launcher design.

This paper introduces a generalized approach to the preliminary design of staged orbital LVs, implemented programmatically in Python as a tool named Adjustable Initial Object-oriented Launcher Optimisation System (AIOLOS) [7]. The tool heavily uses the object-oriented paradigm to provide versatility and the ability to model both expendable and reusable launchers in various configurations, as well as extendibility, to account for the evolving design ideas. AIOLOS optimizes the input LV for payload (P/L) by adjusting the initial assumptions in a loop and seeks a convergent design. The tool cooperates with the DLR in-house aerodynamics tool Calculation of Aerodynamic Coefficients (CAC) [8] and the trajectory tool Staged Rocket Trajectory Optimization and Simulation (STRATOS) [9] to verify some of the assumptions made at the beginning. All three tools are later described in Sec. III.

An algorithm for preliminary LV design should require as few assumptions as possible. One of these pieces of information is the LV mass division into stages, which is represented by their mass ratios μ. The problem of optimal staging has long been researched; Curtis [10] has described it for serially staged launchers, whereas Civek-Coşkun and Özgören [11] have expanded the approach for the general serial and parallel cases, in this paper collectively referred to as the mixed staging. This paper generalizes the aforementioned approaches for possible launcher reusability and develops the method to limit the required unobvious design assumptions.

The AIOLOS-CAC-STRATOS combination applies a design-aerodynamics-trajectory loop with employment of the modified Edberg's design algorithm. This algorithm has been chosen because it is straightforward, easily expandable for cases such as reusability, and applicable to small, medium, and heavy LVs. AIOLOS develops the algorithm by incorporating the possible reusability of an LV into the basic mathematical model and considering it at the calculation of the optimal staging. Hence, it limits the assumptions required from the designer. It also accounts for mixed staging, thus generalizing the procedure for various vertically starting configurations. Regarding the reusability, it considers vertical takeoff and vertical landing (VTVL) launchers and estimates the descent propellant for this case.

To fully address the problem of the preliminary LV design, its mathematical foundations have been expanded, including a) establishment of clear definitions for the LV performance parameters, b) generalization of the mixed optimal staging method for reusability, c) derivation of new dimension- and mass-estimating relations (MERs), and d) formulas for assessment of the descent and dead propellant mass.

The paper first introduces the mathematical model for a generalized staged LV in Sec. II by defining its constituent masses. Subsequently, it establishes definitions and formulas for LV parameters such as structural indices; introduces parameters to account reserve, residual, and descent propellant; and provides formulas for launcher mass calculation (Sec. II.B). Then, the optimal staging problem is described in Sec. II.C, with the applicability of the method of Lagrange multipliers to the previously mentioned generalized LV model for serial, parallel, or mixed-staged LVs. The theoretical part also encompasses the descent propellant mass estimation in Sec. II.D and formulas for delta-v losses in Sec. II.E. The programming implementation of the model, as well as the description of the tools and the design chain, is presented in Sec. III. Finally, the verification of AIOLOS with real launcher data is shown in Sec. IV.A, and the input parameter analysis is shown in Sec. IV.B. The derivations of the formulas from the theoretical part, as well as supplementing tables and figures, are included in the Appendix.

II. Generalized Launch Vehicle Mathematical Model

In this section, the developed mathematical model for the preliminary launcher design is presented. This encompasses basic LV mass and parameter definitions, including adjusted formulas for structural indices, as well as reusability and dead propellant indices. Then, the previously defined LV constituent masses are expressed with these new parameters. Subsequently, the optimal staging problem of a general launcher is described. Finally, the formulas for descent propellant and delta-v estimation are presented and discussed.

In terms of this paper, a model of an LV is referred to as a generalized model if 1) it produces thrust by ejecting its propellant and hence fulfills Tsiolkovsky equation; 2) its stages' thrust and specific impulse remain constant over the course of their flight; 3) it is either expendable or reusable; 4) it consists of N stages in an arbitrary configuration; and 5) its stages, in turn, are composed of components stacked one upon another around a shared, main axis.

Furthermore, reusable launchers are considered in the VTVL configuration. The descent maneuver analyzed in the subsequent sections is the downrange landing. After the stage separation, it 1) follows the ballistic trajectory; 2) executes the reentry burn to decelerate and lowers the maximal stagnation pressure and the heat flux; 3) is subject to aerodynamic braking; and 4) commences the landing burn until the touchdown.

A. Launch Vehicle Mass Definitions

A major part of LV design focuses on its mass distribution, and thus it is necessary to establish clear definitions of all its constituent masses. For both the LV and its stages, the following masses will be defined:

1) **Propellant mass** m_p, which covers the whole flammable substance, both effective (i.e., used to change the impulse of the LV/stage) and dead (i.e., not possible or not originally planned to be used, such as reserve and residual propellant), with constituent masses as follows: a) ideal ascent propellant mass m_p^A; b) ideal descent propellant mass m_p^D; c) ideal total propellant mass $m_p^T = m_p^A + m_p^D$; and d) dead (reserve and residual) propellant mass m_p^R.

2) **Structure mass** m_s, which covers the whole solid construction of the LV: tanks, engines, gimbals, skirts, etc.

3) **Payload mass** m_{PL}, which is understood slightly differently for the LV as a whole and for each of its stages. In the context of an LV, P/L is the object to be put in the aimed trajectory; for a stage, however, P/L means the mass that the stage carries, i.e., the stages above plus the actual P/L; it is noteworthy that the P/L of the uppermost stage equals the P/L of the LV.

The mass definitions are illustrated on an exemplary launcher in a tandem configuration in Fig. 1. Mixed-staged configurations are described later in Sec. II.C.
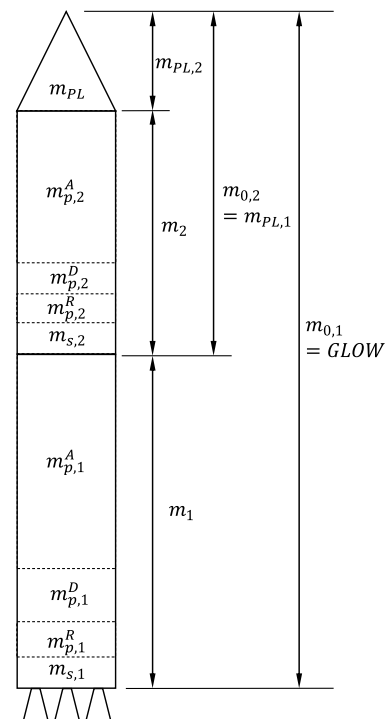

Fig. 1 Launch vehicle mass composition for an exemplary tandem configuration.

Hence, it follows that, for a general reusable or expendable stage with residual propellant, the gross mass m_0 (including P/L) and net mass m (without P/L) equal

$$m_0 = m_s + m_p^T + m_p^R + m_{\text{PL}} = m_s + m_p^A + m_p^D + m_p^R + m_{\text{PL}} \tag{1}$$

$$m = m_s + m_p^T + m_p^R = m_s + m_p^A + m_p^D + m_p^R \tag{2}$$

B. Launch Vehicle Parameters

1. Effective Thrust and Specific Impulse

Parameters crucial for launcher performance include Δv, thrust T, and specific impulse I_{sp}, expressed as

$$\Delta v \triangleq \int_{t_0}^{t_1} \frac{|T(t)|}{m(t)} \, dt = v_{\text{exh}} \ln \mu \tag{3}$$

$$T(t) = v_{\text{exh}}(t) \dot{m}(t) \tag{4}$$

$$I_{\text{sp}} = \frac{v_{\text{exh}}}{g_0} \tag{5}$$

where $T(t)$ and $m(t)$ are, respectively, the stage's thrust and mass as functions of time; v_{exh} is the exhaust gas velocity of the stage engines; and $g_0 = 980{,}665 \text{ m/s}^2$ denotes the standard Earth gravity.

Moreover, Edberg and Costa [6] evoke a useful approximation for the effective specific impulse in the atmosphere $I_{\text{sp-eff}}$, which takes into account the variance in ambient pressure:

$$I_{\text{sp-eff}} = \frac{2}{3} I_{\text{sp-vac}} + \frac{1}{3} I_{\text{sp-SL}} \tag{6}$$

with $I_{\text{sp-vac}}$ and $I_{\text{sp-SL}}$ denoting the specific impulses in vacuum and at sea level, respectively. Under the assumption of constant mass flow $\dot{m}$, the effective thrust equals

$$T_{\text{eff}} = g_0 I_{\text{sp-eff}} \dot{m} = \frac{2}{3} T_{\text{vac}} + \frac{1}{3} T_{\text{SL}} \tag{7}$$

2. Structural Indices

Structural fraction, or structural index, is a measure of the inert (i.e., not propelling) mass in the net stage mass. In aerospace engineering, there are two parallel definitions of the structural index: propellant-based ε and mass-based σ. For the consideration of both reusable and expendable LVs, as well as reserve and residual propellant, a distinction in wet (superscript w) and dry (d) structural indices is made. Wet indices account for the descent and dead propellant mass, whereas dry indices do not take it into consideration; both descent and dead propellant are inert masses during the ascent flight and therefore act similarly to the structure. The indices are hence defined as follows:

$$\sigma^w \triangleq \frac{m - m_p^A}{m} \equiv \frac{m_s + m_p^D + m_p^R}{m_s + m_p^T + m_p^R} \tag{8}$$

$$\sigma^d \triangleq \frac{m - m_p^T - m_p^R}{m} \equiv \frac{m_s}{m_s + m_p^T + m_p^R} \tag{9}$$

$$\varepsilon^w \triangleq \frac{m - m_p^A}{m - m_s} \equiv \frac{m_s + m_p^D + m_p^R}{m_p^T + m_p^R} \tag{10}$$

$$\varepsilon^d \triangleq \frac{m - m_p^T - m_p^R}{m - m_s} \equiv \frac{m_s}{m_p^T + m_p^R} \tag{11}$$

3. Reusability and Dead Propellant Indices

As already mentioned at the beginning of Sec. II, the descent maneuver considered in this paper is the downrange landing of the VTVL configuration.

To effectively analyze the LV mass composition with reusability and dead propellant, it is necessary to define dimensionless parameters that can describe these additional masses in relation to the known masses, just like structural indices relate structure mass to the propellant or net mass of a stage. They will be useful in deriving relations between the structural indices and the mass conversion between virtual and physical stages in the mixed staging problem. These dimensionless parameters are the reusability index ξ and the dead propellant fraction ψ.

Reusability index ξ is defined as the total propellant mass in relation to the ascent propellant mass:

$$\xi \triangleq \frac{m_p^T}{m_p^A} = \frac{m_p^A + m_p^D}{m_p^A} \tag{12}$$

with $\xi = 1$ meaning an expendable stage and $\xi > 1$ meaning a reusable one.

Dead propellant fraction ψ is defined as the dead propellant mass related to the total propellant mass:

$$\psi \triangleq \frac{m_p^R}{m_p^T} = \psi_{\text{reserve}} + \psi_{\text{residual}} \tag{13}$$

It is noteworthy that strictly mathematically ψ must only be greater or equal 0 but does not have an upper limit, because m_p^R is not included in m_p^T. However, the dead propellant mass greater than the combined ascent and descent propellant masses would not constitute a viable, flying LV, and ψ is mostly limited to several percent. Design attempts conducted for this paper and verified with available LV data showed that $\psi_{\text{reserve}}^{\text{default}} = 1\%$ is a sufficient assumption.

The parameter ψ denotes an effective value for a whole stage, which has been done for the sake of simplicity. However, the residual fraction is a property of a tank, not of a stage, so the effective value must be determined from the tanks' properties and from an assumed reserve fraction of the stage:

$$\psi = \psi_{\text{reserve}} + \psi_{\text{residual}} = \psi_{\text{reserve}} + \frac{\psi_f m_f + \psi_o m_o}{m_f + m_o}$$
$$= \psi_{\text{reserve}} + \frac{\psi_f + \varphi \psi_o}{1 + \varphi} \tag{14}$$

where the index f denotes the fuel, the index o denotes the oxidizer, and $\varphi = m_0/m_f$ denotes the oxidizer-fuel mass ratio.

4. Structural Index Relations

The relations between the structural indices are summarized in Table 1. Every relation is specified for a given design, i.e., given ξ and ψ indices.

5. Stage's Constituent Masses

Having calculated or assumed the P/L mass of a stage, its mass ratio, and wet structural index, it can be shown (derivation in Sec. V.B.5) that its ascent propellant mass equals

$$m_p^A = m_{\text{PL}} \frac{\mu - 1}{\xi(\psi + 1)(1 + \varepsilon^d - \mu \varepsilon^w)}$$
$$\equiv m_{\text{PL}} \frac{(\mu - 1)(1 - \sigma^w)}{1 - \mu \sigma^w} \tag{15}$$

Knowing the ascent propellant mass, all other masses can be calculated using Eqs. (2) and (11–13), and the total propellant mass definition from Sec. II.A, with the already present knowledge of the structural index, reusability index, and dead propellant fraction, is as follows:

Table 1   Correlations between structural fractions

	$= f(\sigma^w)_{\xi,\psi}$	$= f(\sigma^d)_{\xi,\psi}$	$= f(\varepsilon^w)_{\xi,\psi}$	$= f(\varepsilon^d)_{\xi,\psi}$
σ^w	σ^w	$1 - \dfrac{1-\sigma^d}{\xi(\psi+1)}$	$1 - \dfrac{1}{\xi\varepsilon^w(\psi+1)+1}$	$1 - \dfrac{1}{\xi(\varepsilon^d+1)(\psi+1)}$
σ^d	$1 - \xi(1-\sigma^w)(\psi+1)$	σ^d	$1 - \dfrac{\xi(\psi+1)}{\xi\varepsilon^d(\psi+1)+1}$	$\dfrac{\varepsilon^d}{\varepsilon^d+1}$
ε^w	$\dfrac{\sigma^w}{\xi(1-\sigma^w)(\psi+1)}$	$1 - \dfrac{1-\xi\psi\sigma^d}{\xi(\psi+1)(1-\sigma^d)}$	ε^w	$1 - \dfrac{1}{\xi(\psi+1)} + \varepsilon^d$
ε^d	$\dfrac{1}{\xi(1-\sigma^w)(\psi+1)}$	$\dfrac{\sigma^d}{1-\sigma^d}$	$\varepsilon^w + \dfrac{1}{\xi(\psi+1)} - 1$	ε^d

$$m_p^D = (\xi - 1)m_p^A \tag{16}$$

$$m_p^T = m_p^A + m_p^D = \xi m_p^A \tag{17}$$

$$m_p^R = \psi m_p^T = \psi\xi m_p^A \tag{18}$$

$$m_p^T + m_p^R = \xi(\psi+1)m_p^A \tag{19}$$

$$m_s = m_p^T(\psi+1)\varepsilon^d \tag{20}$$

$$m = m_p^T + m_p^R + m_s \tag{21}$$

C. Optimal Staging Problem of a Mixed-Staged Launch Vehicle

The optimal staging algorithm by Civek-Coşkun and Özgören [11] allows computing the minimal GLOW of a mixed-staged LV. The algorithm approaches the problem by converting the parallel-staged part of the LV, composed of one central stage (here called the core) and N_b detachable strap-on stages (boosters), into a serially staged part, consisting of two stages, in this paper referred to as the lower virtual stage and the upper virtual stage. The border between both virtual stages is the booster detachment moment; hence, the conversion between the physical and virtual stages does not occur in space, but in time. The lower virtual stage consists of the boosters and the part of the core relevant until detachment, and the upper virtual stage contains the remaining part of the core.

The algorithm does not allow conversion between the physical and the virtual stages, and the mass decomposition of the boosters and the core is unknown. Moreover, this approach does not mention the subject of potential reusability, and it does not account for reserve and residual propellant. Therefore, to consider a serial- or mixed-staged, reusable or expendable LV, a generalization of the approach by Civek-Coşkun and Özgören [11] is needed. The modified method, alongside the mass deconstruction of the virtual stages, is depicted in Fig. 2.

The fundamental idea behind the presented conversion method is the temporal stage composition, and therefore it may also be called the time staging model. Firstly, a clear border between the two virtual stages needs to be drawn; it has already been mentioned that this border shall be the boosters' detachment. Until this moment, both the core and the boosters generate thrust simultaneously. Hence, their equivalent exhaust velocity and specific impulse may be calculated, and they may be treated as one single stage; they constitute the lower virtual stage. Afterward, only the core remains, forming the upper virtual stage. The equivalent parameters are required because both the stage's specific impulse and exhaust gas velocity come into the staging equation.

The problem's intricacy lies in assigning the constituent masses (structure, different propellant types) to the virtual stages. The affiliation of the boosters is simple; their detachment marks the border between the virtual stages, so they belong entirely to the lower virtual stage. Regarding the core stage, after booster detachment, the part of the core that flies further is composed of its structure, remaining ascent propellant, and descent and dead propellants. Hence, the rest, being the ascent propellant burnt until detachment, must be included
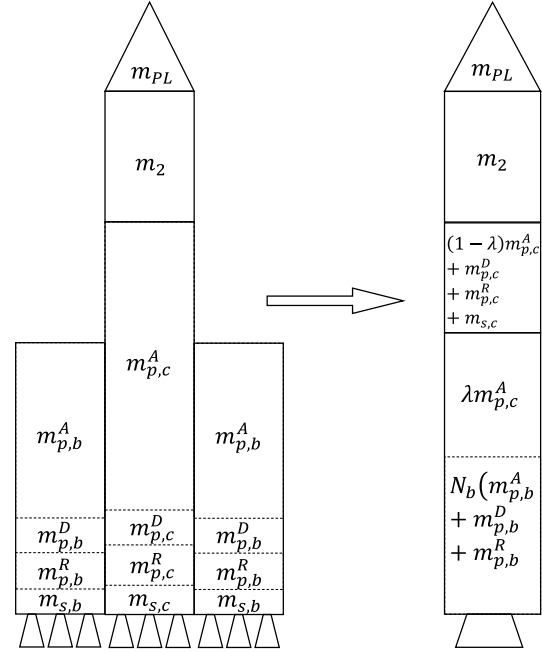

Fig. 2   Conversion from mixed to serial staging with stage mass decomposition; the parameter λ is defined in Sec. II.C.2.

in the lower virtual stage. A rigorous mathematical proof for this consideration can be found in Appendix B.2.

1. Optimization by the Method of Lagrange Multipliers

The main objective of the optimal staging problem is to determine the mass ratios μ of the stages and minimize the theoretical assumed GLOW of a launcher. Curtis [10] has described it for serially staged launchers, whereas Civek-Coşkun and Özgören [11] have expanded the approach for the general serial and parallel cases. In the context of the optimal staging, the variable to be determined is the mass ratio vector of an N-staged launcher, $\boldsymbol{\mu} = [\mu_1 \ \ \mu_2 \ \ \dots \ \ \mu_k \dots \ \ \mu_N]$. Since both expendable and reusable launchers in any staging configuration are considered in this paper, a generalization for these cases as well as a rigorous proof of the method's applicability is needed; detailed mathematical derivations are presented in Appendix B.1. For this purpose, the Lagrange function is defined as follows:

$$\mathcal{L}(\boldsymbol{\mu}, \eta) \triangleq f(\boldsymbol{\mu}) + \eta g(\boldsymbol{\mu}) \tag{22}$$

where η is a Lagrange multiplier, and $f(x)$ denotes the function subjected to the equality constraint $g(x) = 0$. After Civek-Coşkun and Özgören [11], the objective function for the Lagrange equation can be assumed as

$$f(\boldsymbol{\mu}) \triangleq \ell_n \frac{m_0}{m_{PL}} = \sum_{k=1}^{N} \ell_n \frac{\mu_k(1 - \sigma_k^w)}{1 - \mu_k \sigma_k^w} \tag{23}$$

The constraint of the optimization problem is the Tsiolkovsky equation for staged rockets:

$$g(\boldsymbol{\mu}) \triangleq \sum_{k=1}^{N} v_{\mathrm{exh},k} \,\ell n\, \mu_k - \Delta v_{\mathrm{mission}} \tag{24}$$

Thus, the method of Lagrange multipliers with Eqs. (23) and (24) delivers

$$\sum_{k=1}^{N} v_{\mathrm{exh},k} \,\ell n\, \frac{1 + \eta v_{\mathrm{exh},k}}{\eta \sigma_k^w v_{\mathrm{exh},k}} - \Delta v_{\mathrm{mission}} = 0 \tag{25}$$

which is then solved numerically for the Lagrange multiplier η; the Lagrange function formulated for this problem in Eq. (25) will be referred to as the staging equation. Subsequently, knowing η, the mass fraction of the kth stage μ_k can be obtained from Eqs. (23) and (24), supplemented with Lagrange partial derivative constraints $(\partial \mathcal{L}/\partial \eta = 0 \wedge \partial \mathcal{L}/\partial \boldsymbol{\mu} = 0)$, as

$$\mu_k = \frac{1 + \eta v_{\mathrm{exh},k}}{\eta v_{\mathrm{exh},k} \sigma_k^w} \tag{26}$$

As already mentioned in the Introduction, during the first stage of the flight, the boosters and the core generate thrust simultaneously; thus, their specific impulse and exhaust velocity may be brought to equivalent values: specific impulse $I_{\mathrm{sp},1'}$ and exhaust gas velocity $v_{\mathrm{exh},1'}$:

$$\bar{I}_{\mathrm{sp},1'} \equiv \frac{T_{\mathrm{tot}}}{g_0 \dot{m}_{\mathrm{tot}}} = \frac{T_c + N_b T_b}{g_0(\dot{m}_c + N_b \dot{m}_b)} = \frac{T_c + N_b T_b}{\frac{T_c}{I_{\mathrm{sp},c}} + \frac{N_b T_b}{I_{\mathrm{sp},b}}} \tag{27}$$

$$\bar{v}_{\mathrm{exh},1'} \equiv g_0 \bar{I}_{\mathrm{sp},1'} = g_0 \frac{T_c + N_b T_b}{\frac{T_c}{I_{\mathrm{sp},c}} + \frac{N_b T_b}{I_{\mathrm{sp},b}}} \tag{28}$$

After detachment, the remaining upper virtual stage 1" takes over the role of the propelling stage and consists only of the remaining core; therefore,

$$I_{\mathrm{sp},1''} \equiv I_{\mathrm{sp},c} \tag{29}$$

$$\bar{v}_{\mathrm{exh},1''} \equiv v_{\mathrm{exh},c} = g_0 I_{\mathrm{sp},c} \tag{30}$$

2. Parameters of the Virtual Stages

With one core and N_b boosters, the lower virtual stage consists of 1) the entire ascent propellant of the boosters $m_{p,b}^A$; 2) the ascent propellant of the core used until detachment $\lambda m_{p,c}^A$ (coefficient λ is described later in this section); 3) the structure of the boosters $m_{s,b}$; 4) the descent propellant of the boosters $m_{p,b}^D$; and 5) the reserve propellant of the boosters $m_{p,b}^R$.

The upper virtual stage then consists of 1) the remaining ascent propellant of the core $(1 - \lambda)m_{p,c}^A$; 2) the structure of the core $m_{s,c}$; 3) the descent propellant of the core $m_{p,c}^D$; and 4) the reserve propellant of the core $m_{p,c}^R$.

For the analysis of virtual stages, an assumed, nondimensional coefficient λ will be defined, as well as one auxiliary ratio K:

1) λ is the assumed fraction of the core ascent propellant used until booster detachment; this factor sizes the boosters in comparison with the core stage; it follows that it is equivalent to the ratio of the booster burn time $t_{B,b}$ to the core burn time $t_{B,c}$ and can be also expressed with the LV mass decomposition:

$$\lambda \triangleq \frac{m_{p,1',c}^A}{m_{p,c}^A} = \frac{\dot{m}_c t_{B,1',c}^A}{\dot{m}_c t_{B,c}^A} \equiv \frac{t_{B,b}}{t_{B,c}} \tag{31}$$

$$\lambda = \frac{m_{p,1'}^A - N_b m_{p,b}^A}{m_{p,c}^A} \tag{32}$$

2) K is the ratio of the core's ascent propellant to a single booster's ascent propellant; this fraction is defined directly by λ and the parameters of the core and booster engines:

$$K \triangleq \frac{m_{p,c}^A}{m_{p,b}^A} = \frac{\zeta_c}{\zeta_b} \frac{\dot{m}_{p,1'}^A \frac{t_{B,1'}}{\lambda}}{\dot{m}_{p,b}^A t_{B,1'}} = \frac{\zeta_c}{\zeta_b} \frac{1}{\lambda} \frac{T_c/I_{\mathrm{sp},c}}{T_b/I_{\mathrm{sp},b}} \tag{33}$$

where ζ denotes the stage engine's equivalent throttle over its flight ($\zeta = 1$, full thrust for the whole burn time), and t_B is the ascent burn time of a stage.

The staging equation requires knowledge of the stages' gross wet structural indices, as well as their gas exhaust velocities (the latter have already been shown in Eqs. (28) and (30); these are defined as follows:

$$\sigma_{1'}^w \triangleq \frac{N_b(m_{s,b} + m_{p,b}^D + m_{p,b}^R)}{N_b(m_{s,b} + m_{p,b}^R) + \lambda m_{p,c}^A} \tag{34}$$

$$\sigma_{1''}^w \triangleq \frac{m_{s,c} + m_{p,c}^D + m_{p,c}^R}{m_{s,c} + m_{p,c}^D + m_{p,c}^R + (1 - \lambda)m_{p,c}^A} \tag{35}$$

Since the general mixed staging problem divides the stages into virtual ones, their structural indices do not necessarily need to be known and are not trivial to assume. Therefore, formulas to calculate them from the real stages' indices are needed. These formulas, derived in Appendix B.2, are as follows:

$$\sigma_{1'}^w = \frac{\varepsilon_b^w}{\varepsilon_b^w + \frac{1}{\xi_b(\psi_b+1)}\left(1 + \frac{\lambda}{N_b}K\right)} \tag{36}$$

$$\sigma_{1''}^w = \frac{\varepsilon_c^w}{\varepsilon_c^w + \frac{1-\lambda}{\xi_c(\psi_c+1)}} \tag{37}$$

As the conversion between various structural indices requires knowledge of the reusability index and dead propellant fraction of a virtual stage, these can be calculated from their earlier definitions in Eqs. (12) and (13) as follows:

$$\xi_{1'} \triangleq \frac{m_{p,1'}^T}{m_{p,1'}^A} = \frac{\lambda K + N_b \xi_b}{\lambda K + N_b} \tag{38}$$

$$\xi_{1''} \triangleq \frac{m_{p,1''}^T}{m_{p,1''}^A} = \frac{\xi_c - \lambda}{1 - \lambda} \tag{39}$$

$$\psi_{1'} \triangleq \frac{m_{p,1'}^R}{m_{p,1'}^T} = \frac{\psi_b \xi_b}{\lambda K + N_b \xi_b} \tag{40}$$

$$\psi_{1''} \triangleq \frac{m_{p,1''}^R}{m_{p,1''}^T} = \frac{\psi_c \xi_c}{\xi_c - \lambda} \tag{41}$$

The derivations of the presented formulas are shown in Appendices B.2–B.4.

3. Lambda Existence

It can be shown that the previously introduced parameter λ is not allowed to take any arbitrary value from 0 to 1; since it impacts the staging equation and, therefore, the stage mass ratio μ, which cannot be lower than 1, and its actual value range is narrower. Because of the implicit nature of the staging equation, a straightforward relation for λ cannot be derived, and a numerical solution for a given set of specific impulses and structural fractions is needed. An example of
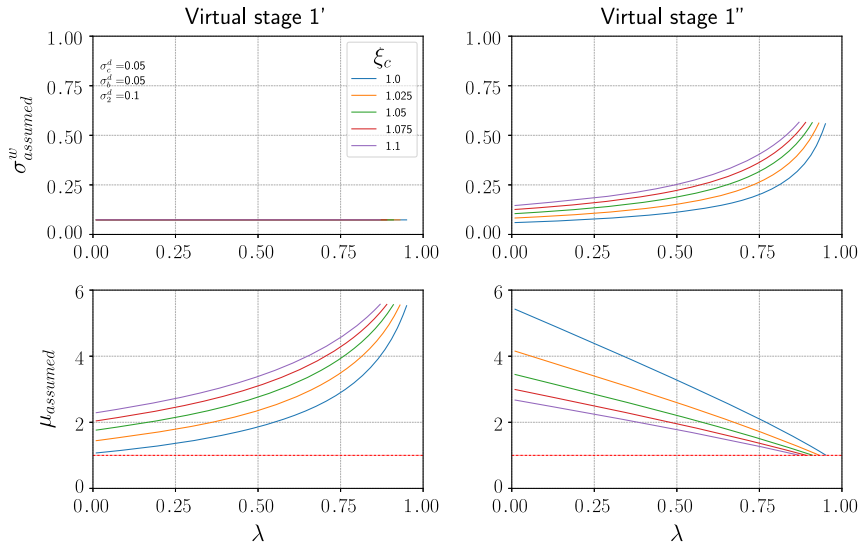
Fig. 3   Lambda existence test for Ariane 5. Red dash-dotted lines denote the lower limit $\mu = 1$.

the numerical λ existence test is depicted in Fig. 3; the test has been performed for Ariane 5 with the following values:

1) Core: $\sigma_c^d = 0.05$, $I_{\text{sp-SL,c}} = 318$ s, $I_{\text{sp-vac,c}} = 429$ s.
2) Boosters: $\sigma_b^d = 0.05$, $I_{\text{sp-eff,b}} = 274, 5$ s.
3) Second stage: $\sigma_2^d = 0.10$, $I_{\text{sp-vac,2}} = 444.6$ s.

The plots show that σ^w and μ assumed at the creation of the virtual stages as functions of the assumed parameter λ. The plots of $\sigma_{\text{assumed}}^w$ of the virtual stages as a function of λ are direct representations of Eqs. (36) and (37). A set of these plots informs a designer of the allowable range of λ and its influence on the parameters of the virtual stages. As expected, $\sigma_{\text{assumed},1'}^w$ remains unaffected by λ because the lower virtual stage does not contain any wet structure of the core; in comparison, λ affects the upper virtual stage, which possesses all of the core wet structure, an effect especially visible for higher λ values. Analogously, μ depends on the propellant fraction in a stage, which explains rising values for the lower virtual stage and sinking values in the upper stage for rising λ.

4.   Limits on the Structural Index

As indicated in Sec. II.C, for the preliminary design of a launcher, its stages' wet structural indices σ_k^w need to be assumed. Therefore, for a better initial choice it is beneficial to know the limits imposed on this parameter. From its definition, it follows that the structural index needs to be between 0 and 1. However, it is subject to another, stricter constraint, which originates from the m_0/m_{PL} ratio, used in the Lagrange objective function from Eq. (23); m_0/m_{PL} ratio cannot be less than 1 for real launch systems:

$$\ell_n \frac{m_0}{m_{\text{PL}}} = \sum_{k=1}^{N} \ell_n \frac{\mu_k(1 - \sigma_k^w)}{1 - \mu_k \sigma_k^w} > 0 \qquad (42)$$

From an analysis of this constraint and the Tsiolkovsky equation, it can be shown that (derivation in Appendix C)

$$\sigma_k^w < \frac{1}{\exp\left(\frac{\Delta v_k}{g_0 I_{\text{sp},k}}\right)} \qquad (43)$$

Furthermore, the ascent propellant mass as a function of σ_k^w can be plotted using Eq. (15), showing that the point $\sigma_k^w = 1/\exp(\Delta v_k/g_0 I_{\text{sp},k})$ is in fact its asymptote; this function is depicted in Fig. 4. The asymptote forms a limit for the structural indices for a particular specific impulse; for structural indices exceeding this limit, the propellant mass becomes negative, which is not physical. By analyzing this limitation, it can be observed that with rising specific impulse the allowable range for structural indices also rises; this means that
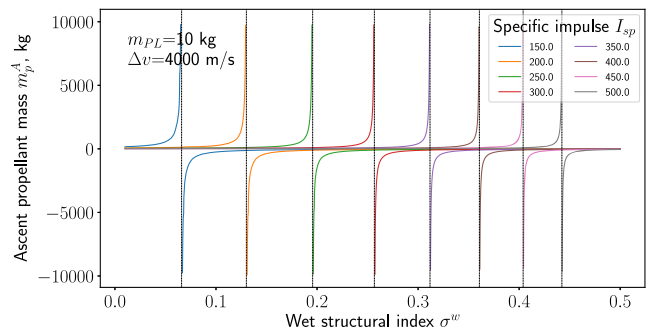

Fig. 4   Ascent propellant mass for a single stage in function of wet structural index and specific impulse for a given delta-v and P/L mass. Dashed vertical lines are the functions' asymptotes.

with more efficient engines, more structural margin is available to the designers.

D.   Descent Propellant Estimation

An essential issue during reusable launcher design is the amount of the descent propellant. The first design iteration, based on assumptions, is especially unobvious; in the case of the ascent propellant, the structural indices and the P/L mass were assumed, the mass ratios were calculated, and on top of these input values the ascent propellant mass was calculated. For the descent, the first idea is to estimate the propellant amount scaled to the ascent propellant mass; this approach is quite commonly used in launcher sizing [12–14], but with different percentages, as collected in Table 2.

The approach by [14] requires a note at this point; though at the beginning it takes an assumed descent propellant mass, it then iterates the design with a trajectory analysis in a loop, and the value in the table is the final one. Therefore, although the mean reusability index equals 1.0888, the default one used in the implementation of the design procedure in AIOLOS is rounded to 0.005 (0.5% of the ascent

Table 2   Statistical estimation of the descent propellant mass

Launcher	m_p^A, t	m_p^D, t	ξ
RETALT [12]	571.50	50.00	1.0875
RETPRO [13]	344.45	55.00	1.1597
H298H77 [14]	280.00	18.00	1.0643
C648C142 [14]	620.80	27.20	1.0438
——	——	Mean value	1.0888

propellant) toward the trajectory-verified values. Thus, the advised reusability index equals 1.085, representing an 8.5% propellant mass addition for the descent. Thus,

$$m_p^D = (\xi - 1)m_p^A \tag{44}$$

$$\xi^{\text{default}} = 1.085 \tag{45}$$

In the scope of this paper, the assumption about the descent propellant amount is verified by simulation in STRATOS (Sec. IV.A.2).

E. Formulas for the Delta-v Losses

The delta-v budget is necessary to be defined at the very beginning of the design process, and since neither the trajectory of a launcher nor its mass is known at this stage, the velocity losses need to be estimated. The delta-v required for a launcher, also called mission delta-v or design delta-v, is composed of the target orbit's velocity and the losses underway:

$$\Delta v_{\text{mission}} = v_{\text{orbit}} + \Delta v_{\text{grav}} + \Delta v_{\text{aero}} + \Delta v_{\text{steer}} + \Delta v_{\text{prop}} - \Delta v_{\text{gain}} \tag{46}$$

where v_{orbit} is the orbital velocity at the perigee, Δv_{grav} denotes the gravitational losses, Δv_{aero} are the aerodynamic drag losses, Δv_{steer} stands for the steering losses, Δv_{prop} denotes the propulsion losses, and Δv_{gain} is the Earth's rotation's assistance at the launch site toward a certain orbit.

Edberg and Costa [6] have explicated the topic of delta-v losses, describing their order of magnitude and overall influence on the mission delta-v, as well as giving several formulas to estimate them at the beginning of a design process. Their order of magnitude and usual values have also been given. Of greatest importance are the gravitational losses, whose typical values lie in the range of 1–2 km/s [6]; next in line are the aerodynamic losses, with usual values of 40–200 m/s [6,15]; lastly, the propulsion and steering losses can vary greatly between launchers, orbits, and trajectories and are in the order of 30–400 m/s [6].

1. Gravitational Delta-v Losses

Edberg and Costa [6] give several formulas for delta-v loss estimation. Gravitational losses can be evaluated as follows:

$$\Delta v_{\text{grav}} = \sqrt{\frac{2g_0 h}{1 + h/R_E}} \tag{47}$$

$$\Delta v_{\text{grav}} = (g_0 t_{B,1} - K_{gg})\left[1 - K_g\left(1 - \frac{1}{\mu_1}\right)\left(\frac{\gamma_{bo}}{90°}\right)^2\right] \tag{48}$$

where h denotes the orbit perigee altitude, R_E is the radius of the Earth, $K_g = f(\Theta, I_{\text{sp-vac},1})$ and $K_{gg} = f(I_{\text{sp-vac},1})$ are empirical coefficients, Θ is the thrust-to-weight ratio, $t_{B,1}$ denotes the burn time of the first stage, μ_1 is the mass ratio of the first stage, and γ_{bo} is an assumed burnout angle (to the horizontal axis) of the first stage.

The first formula [Eq. (47)] is derived from the conservation of energy; it is a rough estimate that does not take into account the duration of the ascent and assumes that the thrust vector is antiparallel to the gravity vector [6]. The second formula [Eq. (48)] [16] is deemed more realistic because it accounts for two factors: the time a vehicle propels against the gravity and the shape of its trajectory. The first factor is expressed in the term $g_0 t_{B,1} - K_{gg}$, where K_{gg} is the correction factor for the overestimation of the losses under the assumption of the constant gravitational field; then, the influence of the trajectory is expressed as the function of the burnout angle, mass ratio, and the correction constant K_G [17]. In this paper, the gravitational losses according to this formula have been calculated only for the first stage, which incurs most of the total gravitational losses; this simplification has delivered quite good results, as will be shown in Sec. IV.A.1.

In the case of Eq. (47), Edberg and Costa [6] remark that it may be convenient for a first, rough estimation, because it does not require any assumptions to make. However, it does not take into account how much time a launcher needs to operate against the gravity force, which in turn depends on its trajectory. It takes a very conservative stance, and therefore, based on the comparison of the two formulas [Eqs. (47) and (48)] on Saturn V, Edberg and Costa [6] advise to account for only 80% of the estimation by Eq. (47). However, as this study has found out, for some launchers, such as RETALT [12,18], 80% is an underestimation, whereas for Falcon FT it results in unrealistically high losses. The deviation was especially perceivable in the case of Falcon FT, where the optimizing analysis suggested a drop in P/L capability to 2.5 t instead of 23 t in the real launcher, because the theoretical formula assessed the gravity losses to be over 2 km/s for low-Earth orbit (LEO), a value significantly overestimated.

The second formula is considered by Edberg and Costa [6] to be far more precise, but its downside is the need of one additional assumption, the first stage's burnout angle γ_{bo}. At no point of the preliminary design analysis (i.e., the run of the algorithm) is the trajectory of the launcher known, and hence it cannot be substituted at any iteration. However, the lack of knowledge of γ_{bo} does not pose a serious problem, because even a significant uncertainty of it does not cause any major error in Δv_{grav}. If γ_{bo} were treated mathematically as a measured quantity with uncertainty of $\Delta\gamma_{bo}$, then the gravity losses uncertainty $\Delta(\Delta v_{\text{grav}})$ could be calculated in accordance with the norm DIN 1319-4 [19] as

$$\begin{aligned} \Delta(\Delta v_{\text{grav}}) &\triangleq \frac{\partial \Delta v_{\text{grav}}}{\partial \gamma_{bo}} \Delta\gamma_{bo} \\ &= \frac{\partial}{\partial \gamma_{bo}}\left[(g_0 t_{B,1} - K_{gg})\left[1 - K_g\left(1 - \frac{1}{\mu_1}\right)\left(\frac{\gamma_{bo}}{90°}\right)^2\right]\right]\Delta\gamma_{bo} \\ &= 2K_g(K_{gg} - g_0 t_{B,1})\left(1 - \frac{1}{\mu_1}\right)\frac{\gamma_{bo}\Delta\gamma_{bo}}{(90°)^2} \end{aligned} \tag{49}$$

For values of $K_g = 0.56 \ 1/\text{deg}^2$, $K_{gg} = 25$ m/s, $t_{B,1} = 180$ s, $\mu_1 = 2.7$, $\gamma_{bo} = 23°$, and $\Delta\gamma_{bo} = 10$ deg, the gravity loss along with its uncertainty equals $\Delta v_{\text{grav}} = (1700 \pm 35)$ m/s; this in turn is equivalent to an error of 2.06%. However, the exact differential linearizes the equation at the measurement point and hence must be examined with caution in cases of significant error, such as $\gamma_{bo} = 23 \pm 10$ deg; the error spans over a significant portion of the γ_{bo} axis, so for boundary values the error might actually be greater than those estimated with the exact differential from Eq. (49), but the gravity loss is still quite insensitive to changes in γ_{bo}; the boundary values for this particular example are $\Delta v_{\text{grav}}(\gamma_{bo} = 13°) = 1727$ m/s and $\Delta v_{\text{grav}}(\gamma_{bo} = 33°) = 1658$ m/s.

The coefficient K_g depends on the thrust-to-weight ratio Θ, so for an optimizing process the aimed thrust-to-weight ratio (TWR) can be assumed. The mass ratio of the first stage is, in turn, known after the first design iteration, and thus K_{gg} is also known. Similarly, the burn time $t_{B,1}$ is also preliminarily known after the first iteration.

Since there were no equations describing the K_g and K_{gg} curves given by Edberg and Costa [6], the curve-fitting procedure of the Python package SciPy was used; the equations were necessary for further implementation and automation in Python. The equations to describe the curves are as follows:

$$K_g(I_{\text{sp-vac}} = 200 \text{ s}) = 0.730325\Theta^{-1.00766} \cdot \ell_n \Theta + 0.405136 \tag{50}$$

$$K_g(I_{\text{sp-vac}} = 300 \text{ s}) = 0.702575\Theta^{-0.81712} \cdot \ell_n \Theta + 0.424864 \tag{51}$$

$$K_g(I_{\text{sp-vac}} = 400 \text{ s}) = 0.745695\Theta^{-0.82590} \cdot \ell_n \Theta + 0.433951 \tag{52}$$

$$K_g(I_{\text{sp-vac}} = 500 \text{ s}) = 0.7930051\Theta^{-0.83491} \cdot \ell_n \Theta + 0.43644 \tag{53}$$

$$K_{gg} = 3.2506 \cdot 10^{-6} \cdot \Theta^{2.79025} - 5.29021 \tag{54}$$

For the coefficient K_g, the data between the curves for different $I_{sp\text{-}vac}$ can be interpolated linearly.

In light of these observations, even though the semi-empirical formula Eq. (48) requires an input that is quite arbitrary and faintly known, it is preferable over the purely theoretical one since it delivers values closer to reality.

2. Propulsion and Steering Delta-v Losses

Regrettably, propulsion and steering delta-v losses (Δv_{prop} and Δv_{steer}) are very difficult to estimate and can vary significantly between orbits, LVs, and trajectories [6]; there are hardly any empirical or statistical formulas to preliminarily calculate them. Nonetheless, since Δv_{prop} and Δv_{steer} encompass a sizeable portion of the launcher's overall delta-v, in range of 30–400 m/s, under any circumstances they can be neglected.

For the purposes of all delta-v analyses, propulsion losses due to specific impulse variation are considered by employing equivalent specific impulse for the lowermost stages of a launcher, which are affected by the changes in ambient pressure. Any equation considering the specific impulse or thrust of the lower stages will follow Eqs. (6) and (7), and therefore Δv_{prop} is considered implicitly and is assumed to be zero.

Steering losses can be estimated with the precise theoretical formula if some simplifying assumptions are made: 1) it is assumed that the first stage flies with the angle of attack (AoA) $\alpha_1 = 0$ and thus does not induce steering losses; 2) the gimbal angle δ equals zero over the whole trajectory; 3) the thrust of the launcher is constant over the flight time of a particular stage; and 4) for the subsequent stages, an equivalent AoA is assumed by the designer (similarly to the angle γ_{bo} at the gravitational losses) and is constant over the whole flight of the upper stages. Based on trajectory analyses of RETALT and Falcon 9 FT (shown in Appendix E), the default value for α for the upper stages has been assumed to be $\alpha_{default} = 20°$; this value is a realistic preliminary value that persists throughout the trajectory for longer periods of time. The mean absolute AoA over time for the two trajectories is also shown in Fig. 5, equaling $13.6103°$ for RETALT and $12.3607°$ for Falcon 9 FT. Hence, the assumption of $\alpha_{default} = 20°$ can be considered conservative; as will be shown in Sec. IV.A.1, this translates to an overestimation of the steering losses.

With all the aforementioned assumptions made, it follows that

$$\Delta v_{steer} = \sum_{k=2}^{N} \int_0^{t_{b,k}} \frac{2T_k}{m_k} \sin^2\left(\frac{\alpha}{2}\right) dt$$

$$= \sum_{k=2}^{N} \int_0^{t_{b,k}} \frac{2T_k}{m_{0,k} - \dot{m}_k t} \sin^2\left(\frac{\alpha}{2}\right) dt$$

$$= \sum_{k=2}^{N} \frac{2T_k \sin^2\left(\frac{\alpha}{2}\right)}{\dot{m}_k} \ell_n \frac{m_{0,k}}{m_{0,k} - \dot{m}_k t_{b,k}} \qquad (55)$$

3. Aerodynamic Delta-v Losses

As for the aerodynamic losses, the formulas by Lobanovsky [20] and Nikishchenko [21] are used, as they deliver much more realistic and consistent results than the one by Edberg and Costa [6] (originally from [22]), while needing less unknown input:

$$\Delta v_{aero} =$$

$$\begin{cases} \left(\dfrac{m_0}{m^*}\right)^{-0.3} \left[0.045 + 0.1(\Theta - 1.17)^{3/2}\right], & \Theta \geq 1.17 \\[3mm] \left(\dfrac{m_0}{m^*}\right)^{-0.3} \left[0.045 + 0.1(1.3332\Theta^2 - 2.9399\Theta + 1.6148)\right], & \Theta \in (1, 1.17) \end{cases}$$

$$(56)$$

with $m^* = 2{,}965{,}241$ kg being the GLOW of the Saturn V launcher for the Apollo 16 mission and Θ denoting the thrust-to-weight ratio.
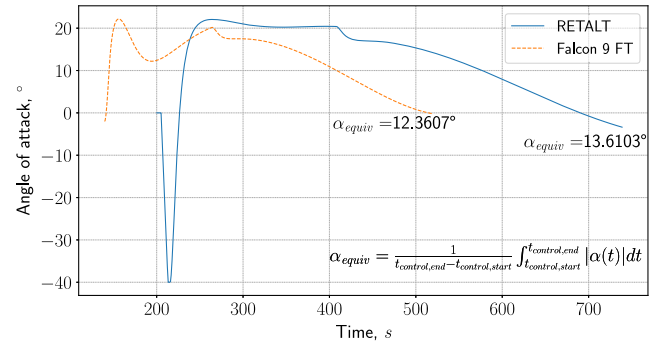

Fig. 5   Angle of attack for RETALT and Falcon 9 FT simulated trajectories from the moment of the control start, with the equivalent values.

Apart from Eq. (47), the formulas for delta-v losses require the knowledge of the LV's GLOW. Equation (47) is a quite conservative estimate of the gravitational losses, the most significant component of the delta-v losses. Therefore, an LV can be preliminarily designed by using exclusively this formula, with aerodynamic and steering losses assumed to be 0; then, the more exact formulas can be employed in the next design iteration.

4. Design Delta-v Margin

Ultimately, the actual design delta-v requires a positive margin to account for inaccuracies in the calculations; the design delta-v of a launcher enhanced by fractional margin χ_v is given as

$$\Delta v_{launcher} = \Delta v_{mission} + \Delta v_{margin} = \Delta v_{mission}(1 + \chi_v) \qquad (57)$$

Computational trials with trajectory verification by STRATOS (Sec. IV.A.1, Table 4) have shown $\chi_v = 1.5\%$ to be an adequate default margin.

III.   Tool Implementation

A. Launcher Design Tool AIOLOS

The main objective of the project was to develop a launcher design algorithm based on as few as possible unobvious assumptions. The algorithm is based mainly on the procedure by Edberg and Costa [6], with additional staging calculations, expansion for reusability, and several other procedures, as described in Sec. II. The algorithm has been implemented in Python 3.11; the created tool is named AIOLOS [7]. As mentioned previously in the paper, special emphasis was put on the tool's versatility and adjustability, in terms of both launcher configurations possible to analyze and the ease of adding new component types, repurposing the program, and expanding it for new technical challenges.

Object-oriented programming was a natural choice for a project this complex because it allows to group similarly behaving parts of code into classes, making the code organized and clear. In AIOLOS, a launcher forms its own class; solid- and liquid-propelled stages are also their own classes. Furthermore, every component type (engine, tank, propellant distribution system, etc.) also constitutes a separate class; some of the components also have subclasses if they behave differently from one another (e.g., fuel tanks and oxidizer tanks or aft and forward skirts are all separate classes).

B. Rapid Aerodynamics Tool CAC

CAC stands for *Calculation of Aerodynamic Coefficients* and is an in-house tool of the DLR for semi-empirical preliminary aerodynamic analysis of LVs [8]. It uses an approach similar to *Missile DATCOM*; CAC describes a launcher's stage parametrically as a serial connection of a conical or ogive nose, a cylinder, and a converging or diverging conical skirt. Then, the aerodynamic coefficients as functions of Mach number and AoA are calculated for the whole launcher based on the superposition of the stages.

C. Trajectory Tool STRATOS

Staged Rocket Trajectory Optimization and Simulation (STRATOS) [9] is a Python tool for 3-degree-of-freedom trajectory simulation developed for multiple-staged launchers and reentry applications for Earth orbits. Core equations are similar to the DLR's TOSCA tool [3,23] and account for changing gravitational field, rotation, and aerodynamic forces. A genetic algorithm is used for the ascent trajectory optimization, maximizing the final velocity of the vehicle for a given orbit perigee. For the descent or reentry trajectory, a gradient-based optimizer is used to define the ignition time and burn duration of a retroboost maneuver to minimize fuel consumption under constrained stagnation pressure, heat flux, and deceleration.

D. AIOLOS-CAC-STRATOS Design Chain

The launcher design chain used to analyze an LV consists of the three tools (AIOLOS, CAC, and STRATOS) coupled together, as visualized in Fig. 6. AIOLOS first calculates the optimal staging for the particular orbit, estimates the masses and geometries of the launcher constituents, and exports the results to CAC and STRATOS. CAC calculates the aerodynamics of the launcher based on the given geometry and creates an aerodynamic database for STRATOS. Finally, STRATOS finds the optimal trajectory for the launcher, which can be used to adjust the input parameters for a better design.

E. AIOLOS Design Procedure and Optimization

Preliminary design of a launcher with a defined P/L mass and aimed orbit in its most basic form includes
1) definition of the launcher parameters and mission;
2) optimal staging determination and the division of delta-v among the stages and hence mass ratiosfirst mass estimations based on assumed structural indices of its stages;
3) calculation of the fuel and oxidizer masses for each stage, including residual and startup propellant;
4) estimations of the components' dimensions, either with statistical or structural formulas (the former ones are available for all component types, and the latter only for some);

5) placing the components in the launcher and calculating their positions;
6) calculations of components' masses, either statistically or with precise formulas for simple shapes;
7) calculations of centers of gravity of the components and then of the stages and of the whole launcher; and
8) calculations of the components', stages', and launcher's moments of inertia.

The procedure can be extended by postdesign functions: a) launcher's mass distribution plot; b) detailed CoG and MoI calculations for different propellant filling percentage; c) CoG and MoI calculations after stages' separation; and d) launcher's visualization (an example shown in Sec. V.E in Fig. E4).

The procedure is possible to be run in a loop to verify some of the initial assumptions. This approach will be referred to as launcher optimization. Firstly, it calculates the launcher's optimal staging based on the input values of the structural index $\sigma_k^{d,\text{assumed}}$ and specific impulse $I_{\text{sp},k}$; then it takes the implicit steps of the design procedure and executes them in two loops:

1) **The inner (or nested) structural loop**: It conducts the rudimentary design procedure, described earlier in this section. Then, it verifies the assumed stage structural indices by comparing the assumed structure mass with the one estimated with MERs, hence producing a certain mass margin $\Delta m = m_s^{w,\text{assumed}} - m_s^{w,\text{real}}$, which is then to be minimized to fit into a given convergence area ($m^{\text{margin},l}$, $m^{\text{margin},u}$). Additionally, it defines a refinement area β_{area} above the upper mass margin, where the numerical step δ_{step} is scaled by the factor β_{step}.

2) **The outer loop**: It verifies the assumed or preliminarily calculated variable (P/L mass, total delta-v, or number of engines) and gradually minimizes or maximizes it until a target thrust-to-weight ratio is achieved within certain convergence area $\epsilon_{\text{TWR}}\text{TWR}^{\text{target}}$. Analogously to the inner loop, the outer loop scales change in the variable with $\Delta\text{TWR} = \text{TWR}^{\text{current}} - \text{TWR}^{\text{target}}$, has a user-defined step, and has a step refinement area β_{area}.

Both the inner and the outer loops are depicted as a block diagram in Fig. 7. The algorithm accepts as input a) the launcher configuration, i.e., the number, type, and ordering of the stages (solid- or liquid-propelled, parallel or serially connected, etc.), and the components' types and ordering inside the stages; b) the initial assumed structural indices of the stages; and c) the initial assumed P/L mass. Regarding the components, their types are defined in the corresponding libraries, and a designer can choose from the available ones or define new components. The definitions are component-specific; for example, for the engines, they encompass their specific impulse (both at the sea level and in vacuum), thrust, chamber pressure, oxidizer-fuel ratio, etc. The output from the algorithm consists of the masses, dimensions, centers of gravity, and moments of inertia of the components, stages, and the launcher.
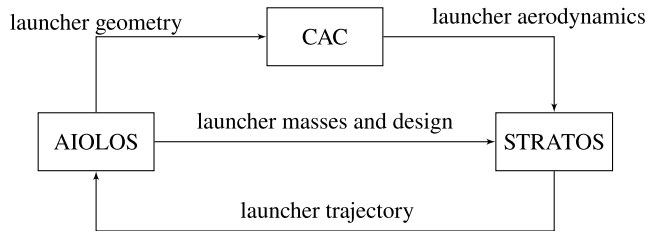
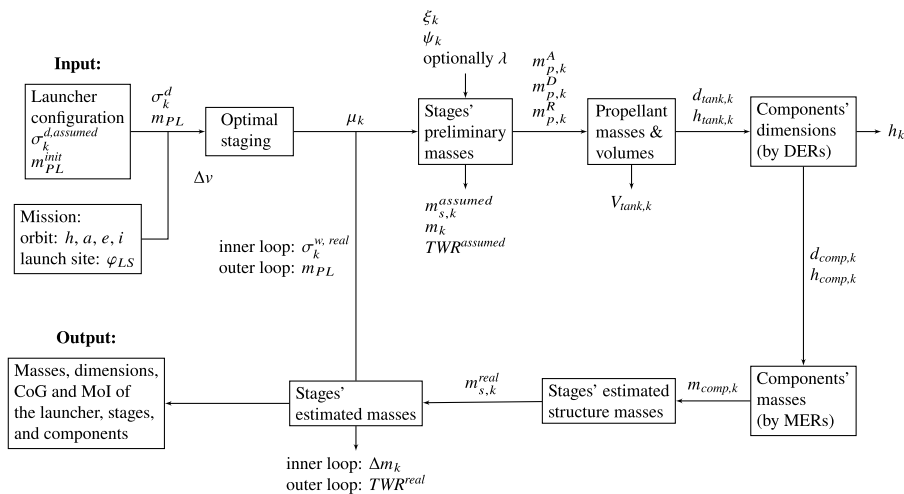

Fig. 6 Design-aerodynamics-trajectory optimization loop.

Fig. 7 Design optimization procedure: the inner loop optimizes the structural index $\sigma_k^{w,\text{real}}$ with mass margin Δm_k as the evaluation function, whereas the outer loop optimizes the chosen variable, like P/L mass m_{PL}, with ΔTWR as the evaluation function.

IV. Results: Tool Verification and Application

A. Launch Vehicle Comparison

To test the correctness of the AIOLOS's output, four launchers have been chosen for a full design procedure in connection with aerodynamics (CAC) and trajectory (STRATOS) analyses. At the end, the simulated trajectories have been compared with the assumed orbits. These particular vehicles have been chosen to test different configurations and orbits with launchers for which ample data are available:

1) RETALT is a partially reusable heavy-lift LV capable of delivering 14.05 t (stage 1 recovered) to geostationary transfer orbit (GTO; 200 km × 35786 km) [12,18].

2) Falcon 9 Full Thrust is a partially reusable medium-lift LV, carrying 18.5 t (stage 1 recovered) to LEO (200 km × 200 km) [24–27].

3) Falcon Heavy is a partially reusable heavy-lift LV with boosters, 57.4 t (boosters recovered) to LEO (200 km × 200 km) [24–27].

4) Ariane 5 ECA is an expendable heavy-lift LV with boosters, delivering 10.8 t to GTO (250 km × 35,786 km) [28–31].

Automatically generated visualizations of RETALT and Ariane 5 ECA are included in Sec. V.E.

1. Ascent Analysis

The output parameters of the launchers modeled with AIOLOS are summarized in Table 3. The entries also show the percentual difference between the outcome from the program and the masses of the real vehicles from the reference sources. All target orbits have the same inclination as the launch site latitude. In the analysis, TWR is the target variable in the optimization for P/L, hence its negligible deviations. RETALT and Falcon 9 FT have been modeled as partially reusable, with their first stages landing on an autonomous drone ship. Falcon Heavy has been modeled with its boosters landing on a drone ship. Furthermore, Falcon 9 and Falcon Heavy need additional clarification; according to their user guide [24], the declared P/L capacity includes the P/L attach fitting, and the exact mission P/L capability can be provided upon request; the reference P/L mass comes from the SpaceX website [32]. The height of Ariane 5 Stage 2 includes P/L fairing (17 m in the reference model).

The first major observation drawn from the comparison is the tendency of AIOLOS to allocate more mass to the uppermost stages of a launcher, which is a direct outcome of the Lagrange staging equation. The launchers show a very promising agreement of the stage net and propellant masses for a preliminary design, showing deviation of no more than 30%. However, for almost all launchers, the structural indices of the lower stages have been underestimated, while those of the upper ones have been overestimated; this indicates a need for improvements in MERs and dimension-estimating relations (DERs) for smaller stages. The largest deviation in structural mass has been shown for Falcon 9 FT, with the structure of the uppermost stage weighing 35% more than the actual launcher.

The model launchers have been investigated with further trajectory analysis in STRATOS, which served as a reference for the delta-v-estimating formulas. The purpose of the analysis was to verify whether the launcher achieves its design orbit with enough velocity. STRATOS uses a trajectory-fixed coordinate system, which means that it is also fixed to the launch site, whereas AIOLOS considers the orbital velocity v_{orbit}, mentioned in Eq. (46), in the geocentric coordinate system; hence, the final velocity from STRATOS for a correct design equals $v_{\text{STRATOS}} = v_{\text{orbit}} - v_{\text{LS}}$. These velocities are summarized alongside the LVs in Table 4.

The results of the AIOLOS-CAC-STRATOS analyses for RETALT, Falcon 9 FT, Ariane 5 ECA, and Falcon Heavy are summarized in Table 4. Furthermore, the mass distribution as well as ascent and descent trajectories of the modeled RETALT and Falcon 9 FT are shown in Appendix E in Figs. E1, E2, and E3. Regarding the trajectories comparison, two notes must be taken:

1) AIOLOS' final orbital velocity equals the theoretical velocity for an elliptic orbit in its perigee.

2) The difference between both analyses is calculated as $\Delta = (v_{\text{AIOLOS}} - v_{\text{STRATOS}})/v_{\text{STRATOS}}$.

There are several observations and notes that can be drawn from the comparative analysis of the delta-v's between AIOLOS and STRATOS:

1) The depicted launchers have been selected from several designs for various input structural indices (and thus various staging); a launcher was required to achieve sufficient final velocity for the aimed orbit, and from the ones that have succeeded in it, the one that delivered the largest P/L was selected for the final statistic.

2) Delta-v has a significant influence on the launcher P/L capability, as depicted in Fig. 8, so it should be assessed as precisely as possible.

3) Gravitational losses have shown a tendency to be underestimated with increasing TWR of a launcher.

Table 3 Masses of the launchers from AIOLOS

Launch vehicle			Stages						
LV	m_{PL}, t	TWR	Stage	m, t	m_p^T, t	m_s, t	σ^d	μ	h, m
Ariane 5 ECA [28–31]	10.30	1.9615	Stage 1	187.63	173.16	10.69	0.0570	— —	30.30
	−4.6%	−1.1%		+1.6%	+1.9%	−27%	−28%	— —	+27%
			Boosters	280.05	245.79	34.26	0.1223	— —	28.57
				+1.1%	+2.4%	−7.4%	−8.4%	— —	−10%
			Stage 2	19.71	14.11	5.30	0.2691	1.8882	25.02
				+1.4%	−5.3%	+17%	+15%	−4.2%	+15%
RETALT [12,18]	14.97	1.2046	Stage 1	693.28	581.95	49.23	0.0710	2.8397	71.83
	+6.5%	+0.1%		−1.8%	−6.4%	−17%	−18%	−12%	+1%
			Stage 2	190.03	171.88	14.72	0.0775	6.1885	36.29
				−6.9%	−8.3%	−12%	−5.3%	−13%	+14%
Falcon 9 FT [24–27]	16.71	1.3628	Stage 1	436.55	410.05	18.30	0.0419	2.9754	47.44
	−10%	+0.6%		−0.4%	−0.2%	−33%	−32%	−16%	16%
			Stage 2	115.80	107.59	6.06	0.0523	5.2995	21.66
				−0.2%	−3.5%	35%	35%	−9.4%	35%
Falcon Heavy [24–27]	50.02	1.5604	Stage 1	439.07	414.85	15.92	0.0363	— —	46.77
	−13%	−1.5%		+1.4%	+1.0%	28%	−29%	— —	+10%
			Boosters	438.75	382.21	15.76	0.0359	— —	50.42
				+1.3%	−7.0%	−29%	−30%	— —	+18%
			Stage 2	124.33	113.45	5.05	0.0406	2.9752	22.98
				+12%	+5.5%	+26%	+13%	+8.2%	+82%

Table 4 Results of the STRATOS trajectory analysis for the exported launchers from AIOLOS

		RETALT	Falcon 9 FT	Ariane 5 ECA	Falcon Heavy
		GTO200	LEO	GTO250	LEO
Payload	AIOLOS	14966	16711	10701	50023
	Reference	14051	18500	10800	57420
	Difference	+6.5%	−10%	−4.6%	−13%
Orbital velocity	Theoretical	10243.1	7787.5	10199.2	7787.5
Launch site gain		463.2	408.6	463.2	408.6
Final velocity	AIOLOS	9779.9	7378.9	9736.0	7378.9
	STRATOS	9755.0	7369.9	9696.3	7396.9
	Difference	+0.3%	+0.1%	+0.4%	−0.2%
Total delta-v	AIOLOS	12173.1	9257.0	11271.5	9011.8
	STRATOS	11962.1	9028.0	12145.9	8659.3
	Difference	+1.8%	+2.5%	−7.2%	+4.1%
Delta-v grav.	AIOLOS	1862.4	1310.6	834.0	1195.7
	STRATOS	1984.3	1481.6	1886.8	1151.5
	Difference	−6%	−12%	−56%	+3.8%
Delta-v aero.	AIOLOS	65.3	86.8	176.8	87.4
	STRATOS	31.7	43.6	63.6	59.8
	Difference	+106%	+99%	+178%	+46%
Delta-v steer.	AIOLOS	465.5	343.9	524.8	351.5
	STRATOS	191.5	133.9	499.4	51.3
	Difference	+143%	+157%	+5.1%	+586%
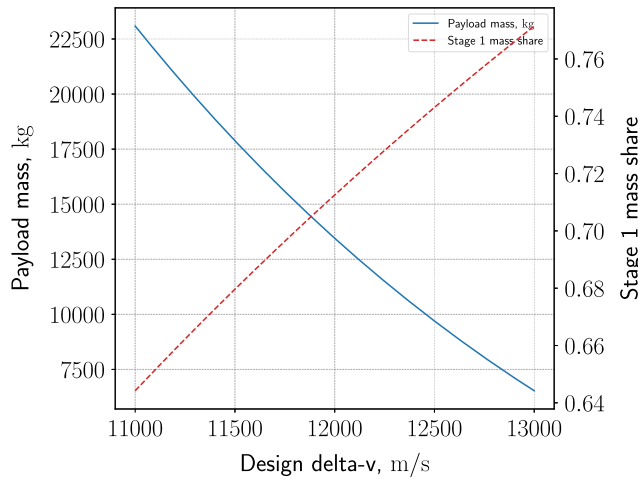
Fig. 8 Influence of the design delta-v of RETALT on P/L mass and first stage mass share.

4) Aerodynamic losses have been generally overestimated; since they form only a small fraction of the delta-v losses, the estimate can be considered acceptable.

5) Steering losses, as predicted, have proved to be quite difficult to estimate accurately; however, the analytical formula from Sec. II.E delivered satisfactory results for the first rough estimate, especially with the trajectory altogether unknown. The steering losses have been overestimated for all investigated configurations due to the conservative assumption of the equivalent AoA. The integrals of the AoA over time, mentioned in Sec. II.E.2 and shown in Fig. 5, suggest that an AoA of 14° could be a less conservative and sufficient assumption.

6) The proposed delta-v margin of 1.5%, mentioned in Sec. II.E.4, has proved to be adequate; it has translated into a positive total delta-v budget for all launchers but Ariane 5 and resulted in correct final velocities for all of them. The final velocity of the launcher was considered the crucial factor in the analysis assessment because it informs about the achieved orbit.

7) Feedback from STRATOS to AIOLOS, forming an iterative mass-trajectory loop, is necessary for an efficient design procedure, providing delta-v and its losses instead of only structural indices, as an input might deliver a more consistent and convergent launcher design.

2. Descent Analysis

Of the four LVs analyzed, three were reusable. Their descent trajectories have been modeled as downrange landing on an autonomous drone ship, with 1) reentry burn, 2) aerodynamic braking, and 3) landing burn. The limiting parameter of the reentry burn was the maximal allowable dynamic pressure (max-q); therefore, the trajectory analyses for different assumed max-q have also been undertaken. An exemplary trajectory as a function of altitude is visible in Fig. 9. The available propellant has been calculated with the assumptions from Sec. II.D. The resulting fuel consumption for the modeled returning stages for different max-q limits has been summarized in Table 5 and shown in Fig. 10. The trajectories of Falcon 9 FT for different max-q are shown in Fig. 11. As described in [9], the heat flux $\dot{q}$ in the stagnation point is calculated from the formula from [33]:

$$\dot{q} = \frac{1}{\sqrt{R_N}} 5.1564 \cdot 10^{-5} \sqrt{\varrho} v^{3.15} \left[\frac{W}{m^2} \right] \tag{58}$$
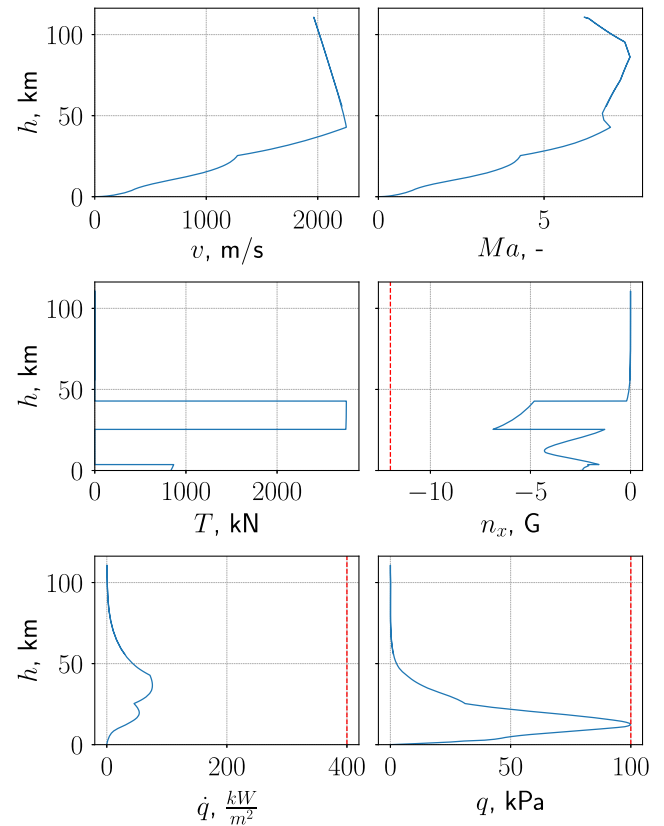

Fig. 9 Falcon 9 FT Stage 1 descent trajectory.

Table 5 Descent propellant consumption of the analyzed reusable LVs

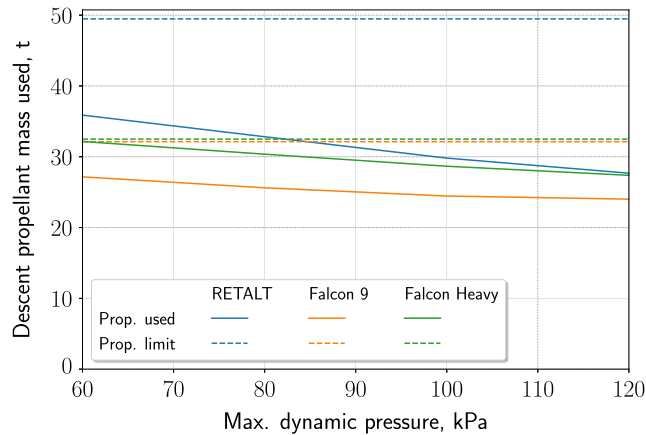| Max. dynamic pressure (q), kPa	Descent propellant mass (m_p^D), t		
	RETALT Stage 1	Falcon Heavy Booster	Falcon 9 FT Stage 1
60	35.88	32.15	27.16
80	32.83	30.36	25.61
100	29.81	28.66	24.45
120	27.68	27.38	24.01
Available	49.47	32.49	32.12

Fig. 10   Descent propellant usage as a function of max. dynamic pressure.
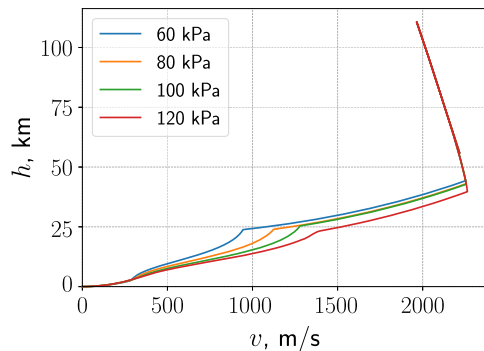

Fig. 11   Falcon 9 FT trajectories for different max-q.

where R_N is the radius of the rounded nose at the stagnation point, ϱ is the ambient air density, and v is the flow velocity.

The available propellant has been overestimated for RETALT (27.5% of the assumed amount still remaining in the tanks for the most conservative assumption of $q_{\max} = 60$ kPa). However, the propellant usage for Falcon 9 FT and Falcon Heavy approached the limit much more closely (15.4 and 1.0%, respectively). The investigated range of maximum dynamic pressures has been chosen conservatively, though; Wilken and Stappert [4] have conducted similar analyses with dynamic pressure at the stagnation point reaching

200 kPa. However, they have imposed stricter constraints on the maximum heat flux (200 kW/m^2) and maximum deceleration (3 g). It is noteworthy that the reentry burn ended at approximately the same altitude of 25–30 km for all cases; similar behavior and similar burn end altitude could be observed in [4].

B.   Parametric Analysis

Since the calculated optimal staging varies in function of the input dry structural indices, a preliminary determination of their values is necessary. In this case, the influence of the input σ_k^d of the stages on the P/L mass, design delta-v, and delta-v losses has been investigated. An example for RETALT is shown in Fig. 12. Every point of the analysis represents a launcher optimized for P/L for the particular set of input σ_k^d.

There are two interesting observations that can be drawn from the analysis:

1) Although gravitational and steering losses, both significant factors in the delta-v budget, have demonstrated altogether different monotonicity, the change in gravitational losses overshadows the steering losses.

2) An extensive test campaign of AIOLOS, coupled with STRATOS, has shown that certain value pairs of σ_k^d theoretically promise the highest payloads, but it does not reflect reality. In this region, the algorithm chooses an unrealistic staging, which translates into the launcher not being able to achieve the orbit with enough velocity, mainly due to an unforeseen rise in all three kinds of delta-v losses; in other words, the loss-estimating equations lose their validity there.

3) For an exemplary RETALT model with input $[\sigma_1^d, \sigma_2^d] = [0.10, 0.05]$, the P/L mass was calculated as 15,243 kg, lying in the region of maximal P/L capacity. However, STRATOS analysis has shown that the launcher would achieve only 8686 m/s instead of the required 9780 m/s, which was caused by the underestimation of the gravity losses by $\Delta v_{\mathrm{grav,STRATOS}} - \Delta v_{\mathrm{grav,AIOLOS}} = 2467$ m/s − 1679 m/s = 788 m/s and the steering losses by $\Delta v_{\mathrm{steer,STRATOS}} - \Delta v_{\mathrm{steer,AIOLOS}} = 815$ m/s − 507 m/s = 308 m/s.

The trajectory analysis has shown that the optimal input structural indices lie roughly in the belt where both design delta-v and theoretical P/L achieve their medians (green in the illustrations), although not in every case the launcher might fly successfully, and several design attempts might be necessary. In this particular case of RETALT modeling, a design has been rendered optimal for the set of $[\sigma_1^d, \sigma_2^d] = [0.088, 0.07]$. The analysis delivers some suggestions for the choice of the indices, but it still leaves too much room for uncertainty and requires time-consuming trajectory simulations.
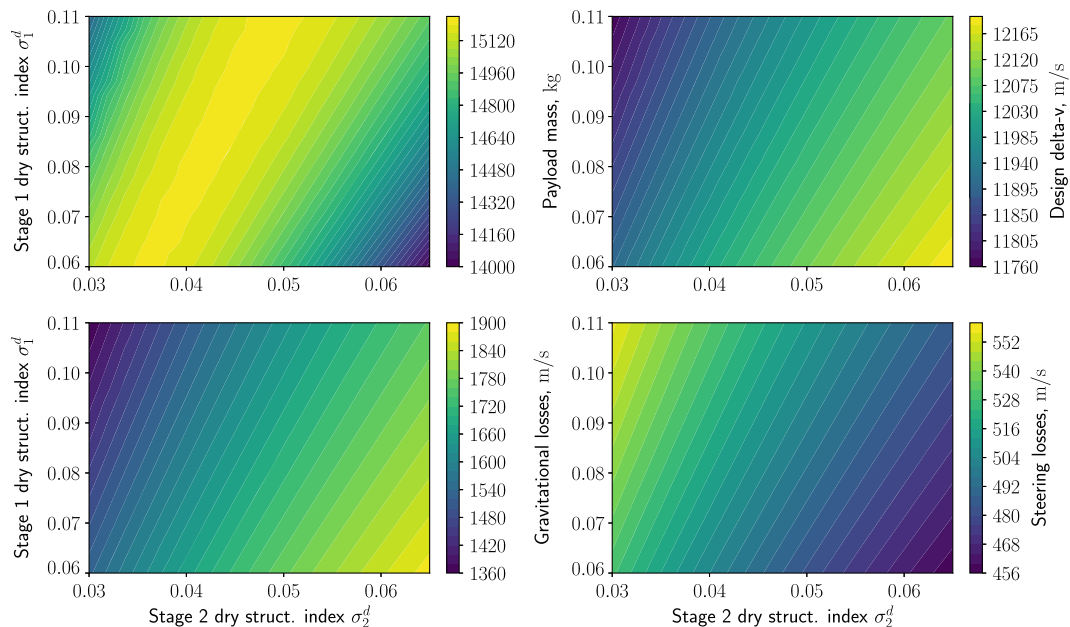

Fig. 12   Influence of the input σ_k^d on the P/L capability and delta-v budget of RETALT.
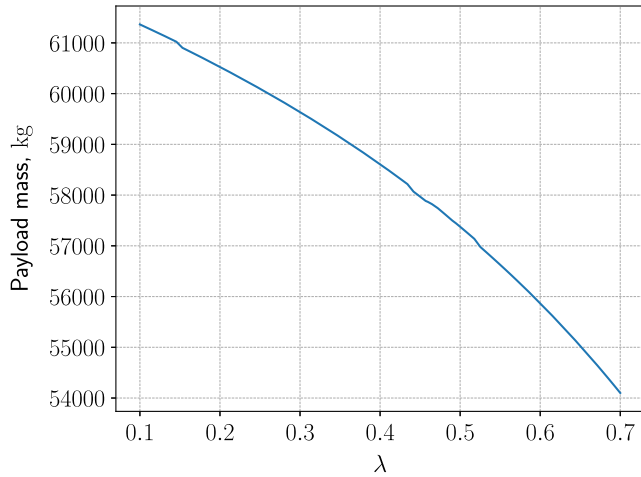
Fig. 13   Influence of the core propellant used until detachment λ on the optimized designs of Falcon heavy.

Fig. 16   Influence of the reusability index of RETALT's first stage on the P/L mass.

Therefore, it needs to be upgraded either by designing reliable feedback without trajectory computation or by improving the time efficiency of the simulation.

The influence of the core propellant used until detachment, λ, on the P/L mass of Falcon Heavy is depicted in Fig. 13. The analysis has been made for the core throttling $\zeta_c = 70\%$ [27].

The parameter λ, although referring explicitly to the core, sizes the boosters as a consequence; it is equivalent to the ratio of the booster to core burn time, $\lambda \equiv t_{B,b}/t_{B,c}$, as shown in Sec. II.C.2. Therefore, the boosters get smaller with the decrease of λ compared to the core. The analysis showed that with the decrease of λ, m_{PL} increases. This suggests that the serially staged configurations may be more efficient, which may explain SpaceX's decision to design the new Starship in a tandem (2-STO) configuration.

Furthermore, the influence of TWR on the P/L mass of Falcon Heavy and RETALT has been investigated, as depicted in Fig. 14. Note that the analysis takes into account the resulting change in estimated delta-v losses; the delta-v's coming from the same analysis for RETALT are depicted in Fig. 15.

These analyses of TWR influence suggest that it is optimal to choose a low TWR for a launcher. The TWR is a scaling factor in this procedure since the number and thrust of the engines are predefined; this means that the launchers with lower TWR are larger. The additional available propellant (and hence longer burn times) for lower TWR outweighs the larger delta-v losses due to higher gravitational losses. It should be noted that this analysis was based on the estimation formulas for the delta-v losses, which lose their validity for very small TWR.

The last discussed analysis is the influence of the reusability index ξ of both stages of RETALT, depicted in Fig. 16. Since ξ is a
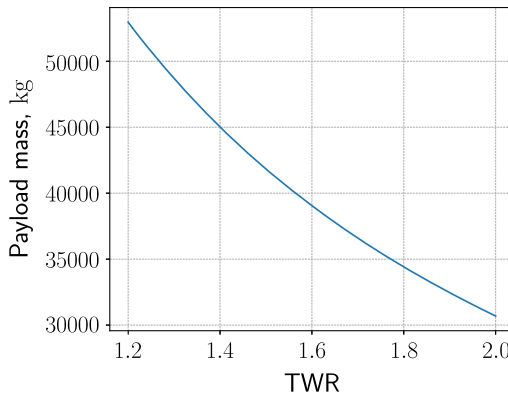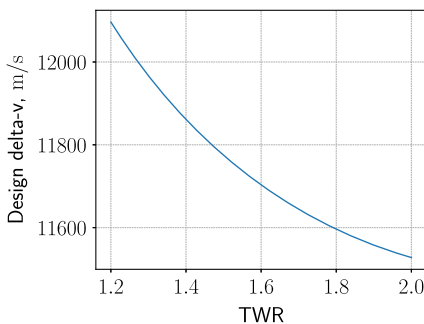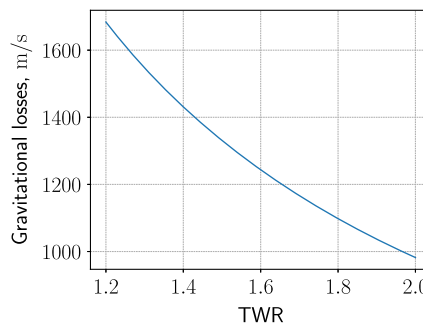
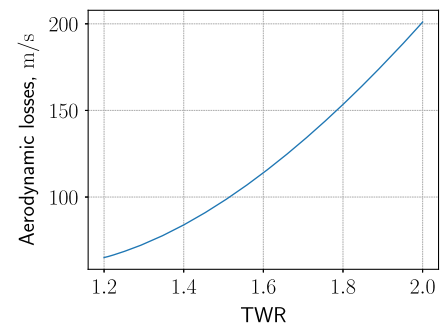**a) Falcon heavy payload mass**
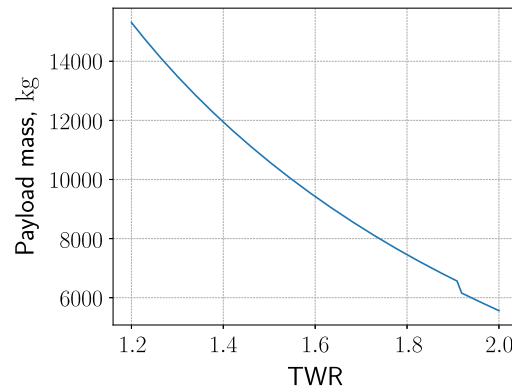
b) RETALT payload mass

Fig. 14   Influence of the thrust-to-weight ratio on the optimized designs of Falcon heavy and RETALT.

a) Total delta-v

b) Gravitational delta-v losses

c) Aerodynamic delta-v losses

Fig. 15   Influence of the thrust-to-weight ratio on the delta-v budget of RETALT. Steering losses have been omitted, as they have barely changed.

parameter introduced in this paper, it is interesting to investigate its influence on the P/L mass, especially since it does not follow straightforwardly from the formulas due to their complexity. The outcome shows that the P/L mass depends linearly on the reusability index, making it easier to preliminarily assess the P/L capability under particular assumptions.

V. Conclusions

In the paper, a preliminary launcher design algorithm has been presented; the algorithm has been implemented as a Python tool named AIOLOS. Behind the tool, there is a launcher design algorithm, devised by Edberg and Costa [6]; it uses DERs and MERs to preliminarily calculate the mass and geometry of the launcher and all its constituents. The algorithm has been further developed: apart from the more detailed launcher decomposition into various components (collected in Appendix Table D1), the reserve, residual, and descent propellants have been considered (Sec. II.B.3), and the number of necessary input assumptions made by a designer has been reduced. This has been achieved by employing the minimization method of Lagrange multipliers to determine the optimal staging, i.e., the optimal division of the launcher's mass into stages. The original method described by [10], further developed by [11] for mixed (serial and parallel) staging, has been generalized (Sec. II.C). This generalization encompasses three main aspects: a) clear definition and recalculation of the stage structural indices, presented in Secs. II.B.2 and II.B.4; b) a detailed method for conversion between physical stages and virtual stages (mathematical constructs used in the Lagrange equation), described in Sec. II.C.2 and shown in Fig. 2; and c) expansion of the method to account for the reusability and for inert and reserve propellant (Sec. II.C.1). The theoretical limits on the structural indices as well as the parameter λ used for the conversion have been investigated in Secs. II.C.4 and II.C.3, respectively.

To complement the design procedure, additional formulas have been researched and investigated for their accuracy. These formulas contain preliminary delta-v loss-estimating relations (Sec. II.E), and DERs and MERs compiled from the literature research as well as devised ad hoc for the paper (Table D1). Furthermore, a formula for the recommended propellant addition for descent flight has been devised statistically from the available launcher data, estimated to be 8.5% of the ascent propellant (Sec. II.D).

To verify the accordance of the launcher mathematical model with reality and the precision of the estimations, a comparison test campaign has been undertaken (Sec. IV.A.1). Four LVs, representing different configurations (number of stages, reusability, usage of boosters, etc.), have been tested coupled with the tools CAC (aerodynamics) and STRATOS (trajectory). The results have shown the following:

1) Good (<7% deviation) P/L capability estimation for RETALT and Ariane 5 is shown, for which the available data were the most precise.

2) The results have shown >10% deviation in *P/L* mass estimation for launchers with fewer available data (Falcon 9 FT and Falcon Heavy).

3) A general tendency of the algorithm (as well as the MERs) to underestimate the structure mass of the launcher is shown; however, the reference data about structure masses themselves have been estimated from third-party reports, not from the launcher's producer, so the actual deviation might actually be lower.

4) A general tendency of the staging optimization to allocate more mass to the upper stages of a launcher is also shown; the suspected reason is that the mass- and dimension-estimating relations show higher deviations from the real-world data for the small upper stages; hence, it could be beneficial to define separate relations for larger and smaller stages to enhance the accuracy of the estimations; this hypothesis would need further investigation in the future.

5) The results have shown a strong dependence of the staging (and, hence, the whole design) on input structural indices σ^d.

The statistical estimation of the required descent propellant has also been verified with trajectory simulations (Sec. IV.A.2). The analysis has shown that the assumed 8.5% should suffice even for a conservative assumption of the allowable dynamic pressure. However, other formulas for the estimation of the heat flux at the stagnation point, such as the modified Chapman equation employed in [4], could be investigated.

Subsequently, an analysis of the input parameter influence has been carried out (Sec. IV.B) in order to investigate the launcher design behavior in response to various initial assumptions. The analysis has shown, e.g., that the decrease of the launcher's thrust-to-weight ratio may prove beneficial.

During the project, many improvement ideas have been postulated. Most crucial is the closer coupling of AIOLOS, CAC, and STRATOS and an improvement in its calculation time. The comparison campaign has shown very promising results for the launchers analyzed with the whole system of these three tools. Especially important is the verification of the initial estimations of the delta-v and its losses; this can be performed by closing the AIOLOS-CAC-STRATOS into a loop, which would provide the necessary feedback.

Moreover, the aforementioned coupling may constitute promising beginnings of larger launcher design software. It could be enhanced with a tool for detailed structural analysis, verifying the launcher's mechanical durability, with information from AIOLOS about its mass composition and STRATOS data on the pressure on the structure. In addition, a tool for economic analysis would prove invaluable in the assessment of the detailed launch financial budget: the launcher's development, manufacturing, and components cost and, subsequently, its cost per kilogram P/L.

Regarding AIOLOS itself, the tool's mass- and dimension-estimating relations might be updated to include the data of the most recent LVs, like Falcon 9. Furthermore, new components might be added to improve the specificity of the analysis. Lastly, the dependence of the optimal staging on the input structural indices could be further analyzed, and its mitigation strategy in the form of an improvement of the algorithm could be developed.

Appendix A: Relations Between Structural Indices

In this section, the derivation of correlations between the four defined structural indices will be shown.

The definitions established in Sec. II.B.2,

$$\sigma^w \triangleq \frac{m_s + m_p^D + m_p^R}{m_s + m_p^T + m_p^R} \tag{A1}$$

$$\sigma^d \triangleq \frac{m_s}{m_s + m_p^T + m_p^R} \tag{A2}$$

$$\varepsilon^w \triangleq \frac{m_s + m_p^D + m_p^R}{m_p^T + m_p^R} \tag{A3}$$

$$\varepsilon^d \triangleq \frac{m_s}{m_p^T + m_p^R} \tag{A4}$$

can be reformulated to relate to ascent propellant mass m_p^A:

$$\sigma^w = \frac{m_s + (\xi-1)m_p^A + \psi\xi m_p^A}{m_s + \xi m_p^A(\psi+1)} \tag{A5}$$

$$\sigma^d = \frac{m_s}{m_s + \xi m_p^A(\psi+1)} \tag{A6}$$

$$\varepsilon^w = \frac{m_s + (\xi-1)m_p^A + \psi\xi m_p^A}{\xi m_p^A(\psi+1)} \tag{A7}$$

$$\varepsilon^d = \frac{m_s}{\xi m_p^A(\psi+1)} \tag{A8}$$

The relations between σ^d and ε^d, obtained by inserting reverted Eq. (A8) into Eq. (A6):

$$\frac{1}{\varepsilon^d} = \frac{\xi m_p^A(\psi + 1)}{m_s} \tag{A9}$$

$$\sigma^d = \frac{m_s}{m_s + \xi m_p^A(\psi + 1)} = \frac{1}{1 + \frac{\xi m_p^A(\psi+1)}{m_s}} = \frac{1}{1 + \frac{1}{\varepsilon^d}} = \frac{\varepsilon^d}{\varepsilon^d + 1} \tag{A10}$$

$$\Rightarrow \varepsilon^d = \frac{\sigma^d}{1 - \sigma^d} \tag{A11}$$

The relations between ε^w and ε^d, obtained by inserting Eq. (A9) into Eq. (A7):

$$\varepsilon^w = \frac{m_s + (\xi - 1)m_p^A + \psi \xi m_p^A}{\xi m_p^A(\psi + 1)} = \frac{m_s + \xi m_p^A - m_p^A + \psi \xi m_p^A}{\xi m_p^A(\psi + 1)}$$
$$= 1 - \frac{m_p^A - m_s}{\xi m_p^A(\psi + 1)} = 1 - \frac{1}{\xi(\psi + 1)} + \frac{m_s}{\xi m_p^A(\psi + 1)}$$
$$= 1 - \frac{1}{\xi(\psi + 1)} + \varepsilon^d \tag{A12}$$

$$\Rightarrow \varepsilon^d = \varepsilon^w + \frac{1}{\xi(\psi + 1)} - 1 \tag{A13}$$

By combining Eq. (A12) with Eq. (A11) it can be shown that

$$\varepsilon^w = 1 - \frac{1}{\xi(\psi + 1)} + \frac{\sigma^d}{1 - \sigma^d} \tag{A14}$$

Subsequently, combining Eqs. (A10) and (A13),

$$\sigma^d = \frac{\varepsilon^d}{\varepsilon^d + 1} = \frac{\varepsilon^w + \frac{1}{\xi(\psi+1)} - 1}{\varepsilon^w + \frac{1}{\xi(\psi+1)}} = 1 - \frac{1}{\varepsilon^w + \frac{1}{\xi(\psi+1)}}$$
$$= 1 - \frac{\xi(\psi + 1)}{\xi \varepsilon^w(\psi + 1) + 1} \tag{A15}$$

Using Eqs. (A9) and (A13), the relations between σ^w, ε^d, and ε^w are as follows:

$$\frac{m_p^A}{m_s} = \frac{1}{\xi \varepsilon^d(\psi + 1)} \tag{A16}$$

$$\sigma^w = 1 - \frac{m_p^A}{m_s + \xi m_p^A(\psi + 1)} = 1 - \frac{\frac{m_p^A}{m_s}}{1 + \xi \frac{m_p^A}{m_s}(\psi + 1)}$$
$$= 1 - \frac{\frac{1}{\xi \varepsilon^d(\psi+1)}}{1 + \frac{1}{\varepsilon^d}} = 1 - \frac{1}{\xi(\varepsilon^d + 1)(\psi + 1)} \tag{A17}$$

$$\Rightarrow \sigma^w = 1 - \frac{1}{\xi \varepsilon^w(\psi + 1) + 1} \tag{A18}$$

From Eq. (A17) it can be shown that,

$$1 - \sigma^w = \frac{1}{\xi(\varepsilon^d + 1)(\psi + 1)} \tag{A19}$$

$$\Rightarrow \varepsilon^d + 1 = \frac{1}{\xi(1 - \sigma^w)(\psi + 1)} \tag{A20}$$

$$\Rightarrow \varepsilon^d = \frac{1}{\xi(1 - \sigma^w)(\psi + 1)} - 1 \tag{A21}$$

Hence, knowing the relations of all other structural fractions with ε^d from Eqs. (A10), (A12), and (A21), it follows that

$$\sigma^d = 1 - \xi(1 - \sigma^w)(\psi + 1) \tag{A22}$$

$$\varepsilon^w = \frac{\sigma^w}{\xi(1 - \sigma^w)(\psi + 1)} \tag{A23}$$

Finally, σ^w can be expressed as a function of σ^d, using Eq. (A22):

$$1 - \sigma^d = \xi(1 - \sigma^w)(\psi + 1) \tag{A24}$$

$$\Rightarrow 1 - \sigma^w = \frac{1 - \sigma^d}{\xi(\psi + 1)} \tag{A25}$$

$$\Rightarrow \sigma^w = 1 - \frac{1 - \sigma^d}{\xi(\psi + 1)} \tag{A26}$$

Appendix B: Optimal Mixed Staging with Reusability

This section considers derivations and proofs of the formulas used for the optimal staging problem and its conversion to real stage masses.

B.1. Lagrange Equation for Optimal Staging with Reusability

As discussed in Sec. II.C.1, the aim of the Lagrange multiplier method in the context of the optimal staging problem is the minimization of the launcher's GLOW m_0; it is done indirectly, by analyzing the GLOW-P/L mass ratio:

$$\frac{m_0}{m_{PL}} = \frac{m_1 + m_2 + m_3 + \ldots + m_N + m_{PL}}{m_2 + m_3 + \ldots + m_N + m_{PL}}$$
$$\cdot \frac{m_2 + m_3 + \ldots + m_N + m_{PL}}{m_3 + \ldots + m_N + m_{PL}} \cdot \ldots \cdot \frac{m_N + m_{PL}}{m_{PL}}$$
$$= \frac{m_1 + m_{0,2}}{m_{0,2}} \cdot \frac{m_2 + m_{0,3}}{m_{0,3}} \cdot \ldots \cdot \frac{m_N + m_{0,N+1}}{m_{0,N+1}}$$
$$= \prod_{k=1}^N \frac{m_k + m_{0,k+1}}{m_{0,k+1}} \tag{B1}$$

where $m_{0,N+1} = m_{PL}$. Invoking the definition of a mass ratio for a general, possibly reusable stage, it follows that

$$m_k = m_{s,k} + m_{p,k}^T + m_{p,k}^R \tag{B2}$$

$$m_{0,k} = m_{s,k} + m_{p,k}^T + m_{p,k}^R + m_{0,k+1} \tag{B3}$$

$$\mu_k = \frac{m_{s,k} + m_{p,k}^T + m_{p,k}^R + m_{0,k+1}}{m_{s,k} + m_{p,k}^D + m_{p,k}^R + m_{0,k+1}} = \frac{1 + \frac{m_{0,k+1}}{m_k}}{\sigma_k^w + \frac{m_{0,k+1}}{m_k}} \tag{B4}$$

$$\Rightarrow \mu_k \sigma_k^w + \frac{m_{0,k+1}}{m_k} \mu_k = 1 + \frac{m_{0,k+1}}{m_k} \tag{B5}$$

$$\Rightarrow \frac{m_{0,k+1}}{m_k} = \frac{1 - \mu_k \sigma_k^w}{\mu_k - 1} \tag{B6}$$

Having inserted the relation above into Eq. (B1), it can be obtained that

$$\frac{m_0}{m_{PL}} = \prod_{k=1}^N \frac{m_k + m_{0,k+1}}{m_{0,k+1}} = \prod_{k=1}^N \frac{1 + \frac{1 - \mu_k \sigma_k^w}{\mu_k - 1}}{\frac{1 - \mu_k \sigma_k^w}{\mu_k - 1}} = \prod_{k=1}^N \frac{\mu_k(1 - \sigma_k^w)}{1 - \mu_k \sigma_k^w} \tag{B7}$$

$$\ell_n \frac{m_0}{m_{PL}} = \sum_{k=1}^N \ell_n \frac{\mu_k(1 - \sigma_k^w)}{1 - \mu_k \sigma_k^w} \triangleq f(\mu_k) \tag{B8}$$

As already mentioned in Sec. II.C.1, the constraining function is the Tsiolkovsky equation for staged rockets:

$$g(\mu_k) \triangleq \sum_{k=1}^{N} v_{\text{exh},k} \, \ell_n \, \mu_k - \Delta v_{\text{mission}} = 0 \qquad (B9)$$

Therefore, the Lagrange function is as follows:

$$\mathcal{L}(\mu_k, \eta) = \sum_{k=1}^{N} \ell_n \frac{\mu_k(1 - \sigma_k^w)}{1 - \mu_k \sigma_k^w} + \eta \left[\sum_{k=1}^{N} v_{\text{exh},k} \, \ell_n \, \mu_k - \Delta v_{\text{mission}} \right] \qquad (B10)$$

To find the extremum, both partial derivatives of the Lagrange function need to be equal zero. The partial derivative $\partial \mathcal{L}/\partial \eta$ is equal $g(\mu_k)$, which already equals zero by definition; hence, only the partial derivative with respect to μ_k need checking:

$$\frac{\partial \mathcal{L}}{\partial \eta} = \frac{1}{\mu_k} + \frac{\sigma_k^w}{1 - \mu_k \sigma_k^w} + \eta \frac{v_{\text{exh},k}}{\mu_k} \overset{!}{=} 0 \qquad (B11)$$

$$\Rightarrow \frac{1 - \mu_k \sigma_k^w + \sigma_k^w \mu_k + \eta v_{\text{exh},k}(1 - \sigma_k^w \mu_k)}{\mu_k(1 - \sigma_k^w \mu_k)} \overset{!}{=} 0 \qquad (B12)$$

$$\Rightarrow 1 + \eta v_{\text{exh},k} - \eta v_{\text{exh},k} \mu_k \sigma_k^w \overset{!}{=} 0 \qquad (B13)$$

$$\Rightarrow \mu_k = \frac{1 + \eta v_{\text{exh},k}}{\eta \sigma_k^w v_{\text{exh},k}} \qquad (B14)$$

By inserting Eq. (B14) into the constraint Eq. (24), the final equation, which is to be solved numerically, is obtained:

$$\sum_{k=1}^{N} v_{\text{exh},k} \, \ell_n \frac{1 + \eta v_{\text{exh},k}}{\eta \sigma_k^w v_{\text{exh},k}} - \Delta v_{\text{mission}} \overset{!}{=} 0 \qquad (B15)$$

This approach has already been undertaken by [10]; however, only tandem configuration was analyzed and then generalized for N stages; neither a rigorous general mathematical proof nor reusability and dead propellant considerations were undertaken.

B.2.   Structural Indices of the Virtual Stages

As mentioned in Sec. II.C.2, the mass-based wet structural index of the lower virtual stage is defined as

$$\sigma_{1'}^w \triangleq \frac{N(m_{s,b} + m_{p,b}^D + m_{p,b}^R)}{N(m_{s,b} + m_{p,b}^T + m_{p,b}^R) + \lambda m_{p,c}^A} \qquad (B16)$$

Using the previously defined coefficients ξ and ψ [Eqs. (12) and (13)],

$$\sigma_{1'}^w = \frac{N_b(m_{s,b} + m_{p,b}^D + m_{p,b}^R)}{N_b(m_{s,b} + (\psi_b + 1)m_{p,b}^T) + \lambda m_{p,c}^A}$$

$$= \frac{N_b(m_{s,b} + m_{p,b}^D + \psi_b m_{p,b}^T)}{N_b(m_{s,b} + m_{p,b}^D + \psi_b m_{p,b}^T) + N_b m_{p,b}^A + \lambda m_{p,c}^A}$$

$$= \frac{1}{1 + \frac{N_b m_{p,b}^A}{N_b(m_{s,b} + m_{p,b}^D + \psi_b m_{p,b}^T)} + \frac{\lambda m_{p,c}^A}{N_b(m_{s,b} + m_{p,b}^D + \psi_b m_{p,b}^T)}}$$

$$= \frac{1}{1 + \frac{1}{\xi_b(\psi_b + 1)} \frac{1}{\varepsilon_b^w} + \frac{\lambda m_{p,c}^A}{N_b m_{p,b}^A \xi_b(\psi_b + 1)} \frac{1}{\varepsilon_b^w}}$$

$$= \frac{1}{1 + \frac{1}{\xi_b(\psi_b + 1)\varepsilon_b^w} \left(1 + \frac{\lambda}{N_b} \frac{m_{p,c}^A}{m_{p,b}^A}\right)}$$

$$= \frac{\varepsilon_b^w}{\varepsilon_b^w + \frac{1}{\xi_b(\psi_b + 1)} \left(1 + \frac{\lambda}{N_b} K\right)}$$

$$\equiv \frac{\varepsilon_b^w}{\varepsilon_b^w + \frac{1}{\xi_b(\psi_b + 1)} \left(1 + \frac{1}{N_b} \frac{\zeta_c}{\zeta_b} \frac{T_c/I_{\text{sp},c}}{T_b/I_{\text{sp},b}}\right)} \qquad (B17)$$

where K is the ratio of the core's ascent propellant to a single booster's ascent propellant, as defined in Sec. II.C.2:

$$K \triangleq \frac{m_{p,c}^A}{m_{p,b}^A} = \frac{\zeta_c}{\zeta_b} \frac{\dot{m}_{p,1'}^A}{\dot{m}_{p,b}^A t_{B,1'}} \frac{t_{B,1'}}{\lambda} = \frac{\zeta_c}{\zeta_b} \frac{1}{\lambda} \frac{T_c/I_{\text{sp},c}}{T_b/I_{\text{sp},b}} \qquad (B18)$$

with $t_{B,1'}$ denoting the burn time of the lower virtual stage (common burn time), and ζ_c, ζ_b meaning engine equivalent throttle during the common burn time ($\zeta = 1$, full thrust) for core and boosters, respectively.

Analogously, from the definition in Eq. (35),

$$\sigma_{1''}^w \triangleq \frac{m_{s,c} + m_{p,c}^D + m_{p,c}^R}{m_{s,c} + m_{p,c}^D + m_{p,c}^R + (1 - \lambda)m_{p,c}^A}$$

$$= \frac{1}{1 + (1 - \lambda) \frac{m_{p,c}^A}{m_{s,c} + m_{p,c}^D + m_{p,c}^R}}$$

$$= \frac{1}{1 + \frac{1 - \lambda}{\xi_c(\psi_c + 1)} \frac{\xi_c m_{p,c}^A(\psi_c + 1)}{m_{s,c} + m_{p,c}^D + \psi_c m_{p,c}^T}} = \frac{1}{1 + \frac{1 - \lambda}{\xi_c(\psi_c + 1)} \frac{1}{\varepsilon_c^w}}$$

$$= \frac{\varepsilon_c^w}{\varepsilon_c^w + \frac{1 - \lambda}{\xi_c(\psi_c + 1)}} \qquad (B19)$$

It is noteworthy here that, from Eq. (B17), $\sigma_{1'}^w$ is independent from λ. This can be explained in the following manner: Since λ is a scaling factor for the pair core-boosters, assuming constant booster mass m_b, and increasing λ, it will only affect the size of the core; therefore, the mass of the lower virtual stage will remain unchanged, and only the upper one will become bigger. This influence is presented in Eq. (B19).

Since a virtual stage is a purely mathematical construct, definition of its structural index is no trivial task whatsoever; its mass composition, presented in Sec. II.C.2, can be assumed in various manners; hence, it requires a strict mathematical proof. To achieve this, the definition of the wet structural index from Eq. (8) needs reformulation in order to make it dependent from a physical quantity well known for a virtual stage; these quantities are the initial and final masses of the stage:

$$\sigma_k^w \triangleq \frac{m_{s,k} + m_{p,k}^D + m_{p,k}^R}{m_{s,k} + m_{p,k}^T + m_{p,k}^R} \equiv \frac{m_{f,k} - m_{0,k+1}}{m_{0,k} - m_{0,k+1}} \qquad (B20)$$

with initial and final masses as defined in Sec. II.A:

$$m_0 = m_s + m_p^T + m_p^R + m_{PL} \tag{B21}$$

$$m_f = m_s + m_p^D + m_p^R + m_{PL} \tag{B22}$$

Subsequently, the aforementioned masses have to be determined for both virtual stages:

$$m_{0,1'} = m_{s,c} + m_{p,c}^A + m_{p,c}^D + m_{p,c}^R$$
$$+ N_b\left(m_{s,b} + m_{p,b}^A + m_{p,b}^D + m_{p,b}^R\right) + m_{0,2} \tag{B23}$$

$$m_{f,1'} = m_{s,c} + (1-\lambda)m_{p,c}^A + m_{p,c}^D + m_{p,c}^R$$
$$+ N\left(m_{s,b} + m_{p,b}^D + m_{p,b}^R\right) + m_{0,2} \tag{B24}$$

$$m_{0,1''} = m_{s,c} + (1-\lambda)m_{p,c}^A + m_{p,c}^D + m_{p,c}^R + m_{0,2} \tag{B25}$$

$$m_{f,1''} = m_{s,c} + m_{p,c}^D + m_{p,c}^R + m_{0,2} \tag{B26}$$

Thus, structural indices for the virtual stages can be calculated as

$$\sigma_{1'}^w = \frac{m_{f,1'} - m_{0,1''}}{m_{0,1'} - m_{0,1''}} = \frac{N_b(m_{s,b} + m_{p,b}^D + m_{p,b}^R)}{N_b(m_{s,b} + m_{p,b}^T + m_{p,b}^R) + \lambda m_{p,c}^A} \tag{B27}$$

$$\sigma_{1''}^w = \frac{m_{f,1''} - m_{0,2}}{m_{0,1''} - m_{0,2}} = \frac{m_{s,c} + m_{p,c}^D + m_{p,c}^R}{m_{s,c} + m_{p,c}^D + m_{p,c}^R + (1-\lambda)m_{p,c}^A} \tag{B28}$$

B.3. Reusability Index and Dead Propellant Fraction of the Virtual Stages

Using the definitions of the reusability index [Eq. (12)] and dead propellant fraction [Eq. (13)], with Eq. (33), and applying it for the virtual stages,

$$\xi_{1'} \triangleq \frac{m_{p,1'}^T}{m_{p,1'}^A} \equiv \frac{m_{p,c,\lambda}^T + N_b m_{p,b}^T}{m_{p,c,\lambda}^A + N_b m_{p,b}^A} = \frac{\lambda m_{p,c}^A + N\xi_b m_{p,b}^A}{\lambda m_{p,c}^A + N m_{p,b}^A} = \frac{\lambda K + N_b \xi_b}{\lambda K + N_b} \tag{B29}$$

$$\xi_{1''} \triangleq \frac{m_{p,1''}^T}{m_{p,1''}^A} \equiv \frac{m_{p,c,1-\lambda}^T}{m_{p,c,1-\lambda}^A} = \frac{(\xi_c - 1)m_{p,c}^A + (1-\lambda)m_{p,c}^A}{(1-\lambda)m_{p,c}^A} = \frac{\xi_c - \lambda}{1-\lambda} \tag{B30}$$

$$\psi_{1'} \triangleq \frac{m_{p,1'}^R}{m_{p,1'}^T} \equiv \frac{m_{p,b}^R}{m_{p,c,\lambda}^T + N_b m_{p,b}^T} = \frac{\psi_b \xi_b m_{p,b}^A}{\lambda m_{p,c}^A + N_b \xi_b m_{p,b}^A} = \frac{\psi_b \xi_b}{\lambda K + N_b \xi_b} \tag{B31}$$

$$\psi_{1''} \triangleq \frac{m_{p,1''}^R}{m_{p,1''}^T} \equiv \frac{m_{p,c}^R}{m_{p,c,1-\lambda}^T} = \frac{\psi_c \xi_c m_{p,c}^A}{(\xi_c - 1)m_{p,c}^A + (1-\lambda)m_{p,c}^A} = \frac{\psi_c \xi_c}{\xi_c - \lambda} \tag{B32}$$

where index c, λ denotes the part of the core burnt until booster detachment, and $c, 1 - \lambda$—from the booster detachment until the core ascent burnout.

B.4. Equivalent Exhaust Velocity

Equivalent specific impulse of the lower virtual stage is defined as

$$\bar{I}_{sp,1'} \triangleq \frac{T_{tot}}{g_0 \dot{m}_{tot}} = \frac{T_c + N_b T_b}{g_0(\dot{m}_c + N_b \dot{m}_b)} = \frac{T_c + N_b T_b}{\frac{T_c}{I_{sp,c}} + \frac{N_b T_b}{I_{sp,b}}} \tag{B33}$$

Hence, the equivalent exhaust velocity of the lower virtual stage equals

$$\bar{v}_{exh,1'} \triangleq g_0 \bar{I}_{sp,1'} = g_0 \frac{T_c + N_b T_b}{\frac{T_c}{I_{sp,c}} + \frac{N_b T_b}{I_{sp,b}}} \tag{B34}$$

The upper virtual stage 1″ consists only of the remaining core; therefore,

$$\bar{v}_{exh,1''} \triangleq g_0 I_{sp,1''} = g_0 I_{sp,c} \tag{B35}$$

B.5. Propellant Mass of a Serially Connected Stage

The propellant mass of a serially connected stage, which the conversion into virtual stages aims for, with the parameters ψ and ξ, can be derived from its P/L mass and structural indices ε^w and ε^d:

$$\mu \triangleq \frac{m_0}{m_f} = \frac{m_s + m_p^A + m_p^D + m_p^R + m_{PL}}{m_s + m_p^D + m_p^R + m_{PL}} \tag{B36}$$

$$\Rightarrow \mu[m_s + m_p^D + m_p^R + m_{PL}] = m_s + m_p^A + m_p^D + m_p^R + m_{PL} \tag{B37}$$

$$\mu[\xi(\psi + 1)\varepsilon^w m_p^A + m_{PL}] = \xi(\psi + 1)\varepsilon^w m_p^A + m_p^A + m_{PL} \tag{B38}$$

$$m_p^A[1 + \varepsilon^w \xi(\psi + 1) - \mu\varepsilon^w \xi(\psi + 1)] = m_{PL}(\mu - 1) \tag{B39}$$

$$\Rightarrow m_p^A = m_{PL}\frac{\mu - 1}{1 - \varepsilon^w \xi(\psi + 1)(\mu - 1)} \equiv m_{PL}\frac{(\mu - 1)(1 - \sigma^w)}{1 - \sigma^w \mu} \tag{B40}$$

The latter equivalence comes from the relation between ε^w and σ^w [Eq. (A23)].

B.6. Masses of the Member Stages of the Virtual Stages

Having an auxiliary parameter M introduced,

$$M \triangleq \frac{m_c}{m_b} = \frac{m_{s,c} + m_{p,c}^T + m_{p,c}^R}{m_{s,b} + m_{p,b}^T + m_{p,b}^R}$$
$$= \left[\frac{\varepsilon_c^d \xi_c(\psi_c + 1) + \xi_c(\psi_c + 1)}{\varepsilon_b^d \xi_b(\psi_b + 1) + \xi_b(\psi_b + 1)}\right]\frac{m_{p,c}^A}{m_{p,b}^A}$$
$$= \frac{\xi_c(\varepsilon_c^d + 1)(\psi_c + 1)}{\xi_b(\varepsilon_b^d + 1)(\psi_b + 1)}K \tag{B41}$$

it can be derived that

$$m_{1'} + m_{1''} = m_c + N_b m_b = m_c\left(1 + \frac{N_b}{M}\right) \tag{B42}$$

$$\Rightarrow m_c = \frac{m_{1'} + m_{1''}}{1 + \frac{N_b}{M}} \tag{B43}$$

$$\Rightarrow m_b = \frac{m_c}{M} \tag{B44}$$

Furthermore, knowing the net mass of a physical stage, their propellant masses can be derived from Eq. (A8):

$$\varepsilon^d = \frac{m_s}{\xi m_p^A(\psi + 1)} \tag{B45}$$

$$m = m_s + \xi(\psi + 1)m_p^A \tag{B46}$$

$$m = \varepsilon^d(\psi + 1)m_p^A + \xi(\psi + 1)m_p^A \tag{B47}$$

$$m_p^A = \frac{m}{(\psi + 1)\varepsilon^d \xi} \tag{B48}$$

Appendix C: Limits on the Structural Index

As mentioned in Sec. II.C.4:

$$\ell n \frac{m_0}{m_{\mathrm{PL}}} = \sum_{k=1}^{N} \ell n \frac{\mu_k(1-\sigma_k^w)}{1-\mu_k\sigma_k^w} > 0 \tag{C1}$$

$$\Rightarrow \ell n \frac{\mu_k(1-\sigma_k^w)}{1-\mu_k\sigma_k^w} > 0 \tag{C2}$$

$$\Rightarrow \frac{\mu_k(1-\sigma_k^w)}{1-\mu_k\sigma_k^w} > 1 \tag{C3}$$

for every stage k. Equation (C3) can be split into two sets of inequalities to analyze

$$1-\mu_k\sigma_k^w > 0 \wedge \mu_k(1-\sigma_k^w) > 0 \tag{C4}$$

$$\text{or}$$

$$1-\mu_k\sigma_k^w < 0 \wedge \mu_k(1-\sigma_k^w) < 0 \tag{C5}$$

Equation (C5) is never fulfilled because $\mu_k > 1 \wedge \sigma_k^w < 1 \Rightarrow \mu_k(1-\sigma_k^w)$, which is the second requirement in Eq. (C4); therefore, its first part need to be analyzed:

$$1-\mu_k\sigma_k^w > 0 \tag{C6}$$

$$\mu_k\sigma_k^w < 1 \tag{C7}$$

$$\sigma_k^w < \frac{1}{\mu_k} = \frac{1}{\exp\left(\frac{\Delta v_k}{g_0 I_{\mathrm{sp},k}}\right)} \tag{C8}$$

Appendix D: Dimension and Mass-Estimating Relations Compilation

The DERs and MERs, compiled in Table D1, come from various publications ([6,34–37]), referenced next to a component's name. Input values are to be in SI units without prefixes. Grid fins and landing gear are additionally shown in Figs. D1a and D1b, respectively; their geometries have been modeled according to [7,38].

Table D1   Dimension and mass-estimating relations (DERs and MERs)

Component	Geometric model	DER	MER
Payload fairing (PF) [6,34] booster cap	Thin cone of height h_{cone} and optionally a thin cylinder of height h_{cyl} underneath	$h_{\mathrm{cone}} = 2d_{\mathrm{st}}$ (m) h_{cyl} user-defined	$m = k_{PF}A$ (m²) $k_{\mathrm{PF,metal}} = 13,3\,\frac{\mathrm{kg}}{\mathrm{m}^2}$ $k_{\mathrm{PF,composite}} = 9,89\,\frac{\mathrm{kg}}{\mathrm{m}^2}$
Payload attach fitting (PAF) [35]	Point mass	$h = 0$	$m = 0.0755 m_{\mathrm{PL}}$(kg) $+ 50$ kg
Skirt [34]	Thin cylinder of height h_{cyl}	Forward and aft skirt: $h_{\mathrm{cyl}} = \frac{1}{3}d_{\mathrm{st}}$ (m) $+ h_{\mathrm{dome}}$ (m) lowermost aft skirt: $h_{\mathrm{cyl}} = d_{\mathrm{st}}$ (m)	$m = 13,3\,\frac{\mathrm{kg}}{\mathrm{m}^2}A$ (m²)
Avionics [6]	Point mass	$h = 0$	$m_{\mathrm{PL}} < 1$ t: $m = 75$ kg $m_{\mathrm{PL}} \geq 1$ t: $m = 350$ kg 80% in the uppermost stage, 20% distributed among remaining stages
Wiring [6]	Thin bar	$h = h_{\mathrm{st}}$ (m)	$m = 1,43\,\frac{\mathrm{kg}}{\mathrm{m}}h_{\mathrm{st}}$ (m)
Engines [6]	Thin cone frustum of height h_{engine} upper diameter d_{chamber} lower diameter d_{exit}	h_{engine}, d_{chamber}, and d_{exit} user-defined	$m = T(\mathrm{N})\left(7,81 \times 10^{-4} + 3,37 \times 10^{-5}\sqrt{\frac{A_{\mathrm{exit}}}{A_{\mathrm{throat}}}}\right)\frac{\mathrm{kg}}{\mathrm{N}} + 59$ kg
Propellant tank [34]	Convex–convex, convex–concave, or concave–convex cylindrical tank with cylindrical part of the height h, or a spherical tank	Cylindrical: $d = d_{\mathrm{st}}$ $A = \pi d^2 + \pi dh$ convex–convex: $h = \frac{4}{\pi d^2}\frac{V_p}{n} - \frac{\pi d^3}{6AR}$ concave–convex / convex–concave: $h = \frac{4}{\pi d^2}\frac{V_p}{n}$ spherical: $d = \sqrt[3]{\frac{6V_p}{n\pi}}\ A = \pi d^2$	Statistical: $m = k_{\mathrm{con}}m_{\mathrm{con}}$ (kg) RP-1: $k_{\mathrm{con}} = 0.0148$ LOx: $k_{\mathrm{con}} = 0.0107$ LH2: $k_{\mathrm{con}} = 0.1280$ LCH4: $k_{\mathrm{con}} = 0.0288$ structural (Barlow's formula): $m = A\delta$ $p_{\mathrm{tot}} = p_{\mathrm{press}} + \varrho_{\mathrm{con}}hg_0 + (\mathrm{TWR} - 1)$ $N_{\mathrm{circ}} = p_{\mathrm{tot}}\frac{d}{2}$ $N_{\mathrm{ax}} = \frac{p_{\mathrm{tot}}\frac{\pi d^2}{4}}{\pi d}$ $\delta = \frac{\sqrt{N_{\mathrm{circ}}^2 + N_{\mathrm{ax}}^2}}{\sigma_{\mathrm{yield}}}$

Table D1 (*Continued.*)

Component	Geometric model	DER	MER
Fuel[a] [6]	Fluid enclosed in a tank	$V = \dfrac{m_f}{\varrho_f}(1 + u_f + s_f)$ $u_f = 0.03$ RP-1: $s_f = 0$ LH2: $s_f = 0.0143$ LCH4: $s_f = 0.0143$	$f_f = \dfrac{\varphi}{1 + \varphi}$ $m = (m_p^T + m_p^R)f_f + \dot{m}_p t_{startup}f_f$
Oxidizer [6]	Fluid enclosed in a tank	$V = \dfrac{m_o}{\varrho_o}(1 + u_o + s_o)$ $u_o = 0.03$ LOx: $s_o = 0.0143$	$f_o = \dfrac{1}{1 + \varphi}$ $m = (m_p^T + m_p^R)f_o + \dot{m}_p t_{startup}f_o$
Pressurization gas [5]	Gas in a spherical tank	$V = \dfrac{mRT}{p_{press}}$	$m = 1.1\dfrac{p_{ullage}V_p}{RT}\dfrac{\varkappa}{1 - \dfrac{p_{ullage}}{p_{press}}}$
Pressurization liquid [5][b]	Liquid in a spherical tank	$V = \dfrac{m}{\varrho(T)}$	$m = 1.1\dfrac{p_{ullage}V_p}{RT}$
Pressurization tank [5]	Spherical tank	$d = \sqrt{\dfrac{3V_{fluid}}{\pi}}$ for gas: $\delta = 2\dfrac{p_{press}R}{2\sigma_{yield}}$ for liquid: $\delta = 4$ mm	$m = \pi D^2 \delta\varrho_{press.tank}$
Tank insulation [6]	Thin shell around a tank	$V = 0$	$m = k_{ins}A$ $k_{ins} = -1.077\,\ell_n\,\Delta T + 6.0649\,\dfrac{\text{kg}}{\text{m}^2}$
Solid rocket motor (SRM) casing [34]	Convex–convex cylindrical tank	$V = 1.12V_{content}$	$m = k_{casing}m_{content}(\text{kg})$ steel: $k_{casing} = 0.1350$ composite: $k_{casing} = 0.1154$
Intertank structure [34]	Thin cylinder	$h = \dfrac{1}{4}d_{st} + 2h_{dome}$	$m = 13,3\,\dfrac{\text{kg}}{\text{m}^2}A(\text{m}^2)$
Thrust structure [34]	Solid cylinder	$h = \dfrac{2}{3}d_{st} - h_{dome}$	$m = 2.55 \times 10^{-4}\,\dfrac{\text{kg}}{\text{N}}T(\text{N})$
Gimbals [6]	Point mass	$h = 0$	$m = 237.8\left[\dfrac{T(\text{N})}{p_{chamber}(\text{Pa})}\right]^{0.9375}$
Interstage [34]	Thin cone frustum	Hemispherical domes: $h = \dfrac{5}{4}d_{st}$ elliptical-hemispheroid domes: $h = d_{st}$	$m = 13,3\,\dfrac{\text{kg}}{\text{m}^2}A\,(\text{m}^2)$
Propellant distribution system (PDS) [36][c]	Two opposite thin bars of heights h_1 and h_2[d]	$h_1 = \dfrac{1}{2}h_{st}, d_1 = \sqrt{\dfrac{4\dot{m}_1}{\pi\varrho_1 v_{fl}}}$ $h_2 = h_{st}, d_2 = \sqrt{\dfrac{4\dot{m}_2}{\pi\varrho_2 v_{fl}}},$ $v_{fl} = 10\,\dfrac{\text{m}}{\text{s}}$	$m = 2.1727\,\dfrac{\text{kg}}{\text{m}^2}\pi d_{st}\,(\text{m})h_{st}\,(\text{m})$
Hydraulics [36][e]	Point mass	$h = 0$	$m = 0.0023m_{0,st}$
Stage separation mechanism (SSM) [37]	Point mass	$h = 0$	$m = 8.7 \times 10^{-4}m_{PL,st}$
Grid fins [7]	Geometry in Fig. D1(a)	$a_{init} \approx 0.4d_s$ $b_{init} \approx \dfrac{9}{11}a$ $n_a = \text{round}(a_{init}l_s\sqrt{2})$ $n_b = \text{round}(b_{init}l_s\sqrt{2})$ $a = n_a(l_s + t)\sqrt{2}$ $b = n_b(l_s + t)\sqrt{2}$	$m = \varrho\delta[ab - 2n_a n_b l_s^2 + 2(a + b - 2t)t + 2at_b]$
Landing gear [7]	Geometry in Fig. D1(b)	$l = d_s$ $h_A = \dfrac{d_s}{2}$ $h_B = d_s$	$m = 0.09m_{s,st}$

[a]Engine startup time $t_{startup} = 2$ s [6].
[b]Model by [5] modified for a liquid.
[c]MER by [36]; DER devised ad hoc for the paper.
[d]Index 1 refers to the lower tank in the stage, and 2 to the upper ($\dot{m}_f = \dot{m}_p/1 + \varphi, \dot{m}_o = \dot{m}_p/1 + 1/\varphi$).
[e]Original MER fitted to Space Shuttle; the given one is fitted to RETALT.
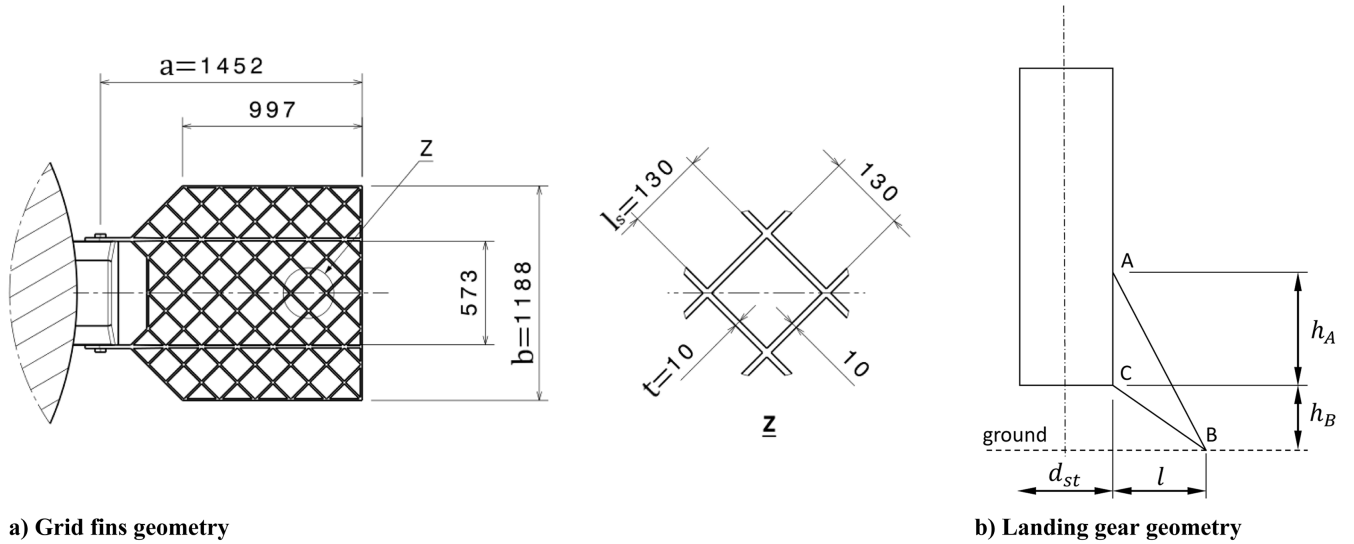
a) Grid fins geometry

b) Landing gear geometry

**Fig. D1   Grid fins [38] and landing gear [7] geometries.**

Indices used: PF, P/L fairing; st, stage; press, pressurization; ins, insulation; con, contents; p, propellant; f, fuel; o, oxidizer; startup, engine startup time; circ, circumferential; ax, axial; tot, total.

Variables: A, outer surface area of a component; T, single engine thrust; V_p, propellant volume; φ, oxidizer-to-fuel ratio; AR, dome aspect ratio; n, number of components; R, individual gas constant; $\varkappa$, gas adiabatic index; T, temperature; p, pressure; δ, wall thickness; σ_{yield}, yield stress; ΔT, temperature difference between neighboring tanks; $\dot{m}_1$, mass flows from the lower tank in the stage; $\dot{m}_2$, mass

flows from the upper tank in the stage; ϱ, fluid density; u, ullage factor; s, shrinkage factor; f, mix ratio; ψ, dead propellant fraction; ξ, reusability index; N, force flux.

Appendix E: Launcher Mass Composition, Trajectories, and Visualizations

An exemplary mass compositions of RETALT and Falcon 9 FT are shown in Fig. E1. Trajectories of the analyzed RETALT and Falcon 9
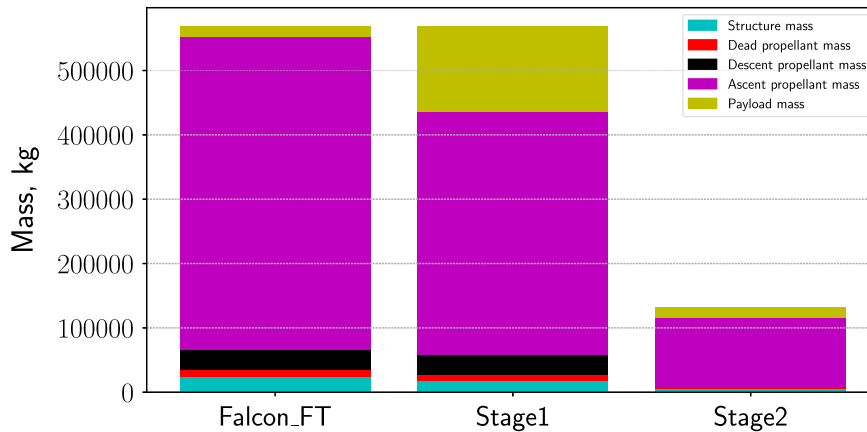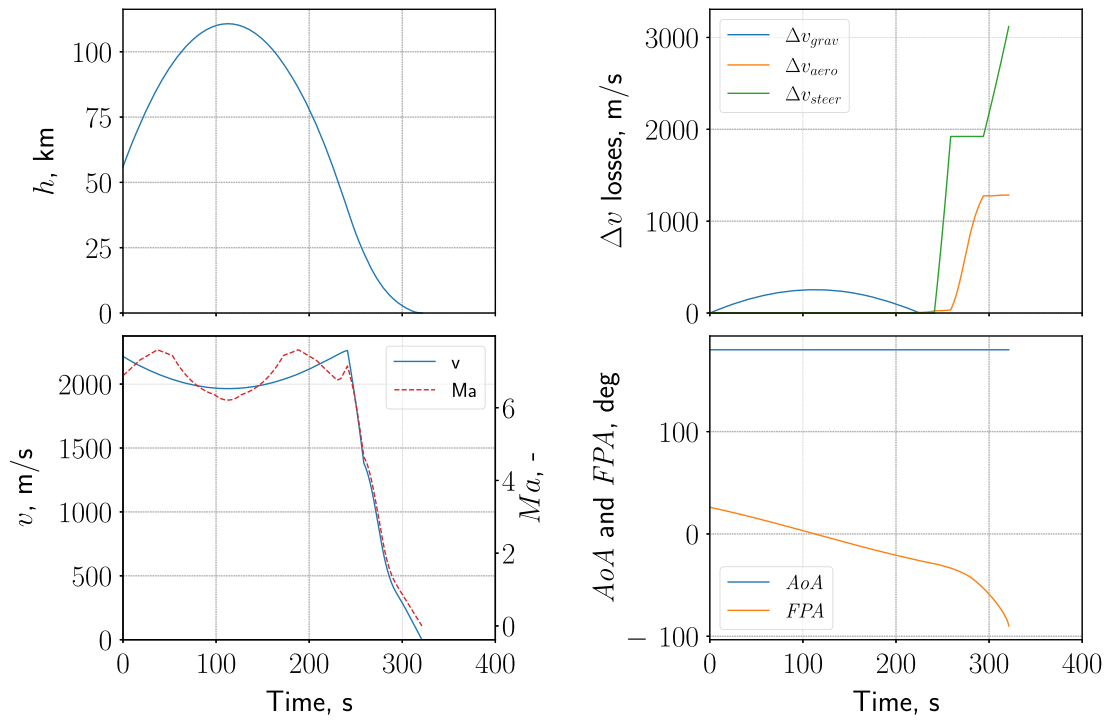

a) Falcon 9 FT mass composition
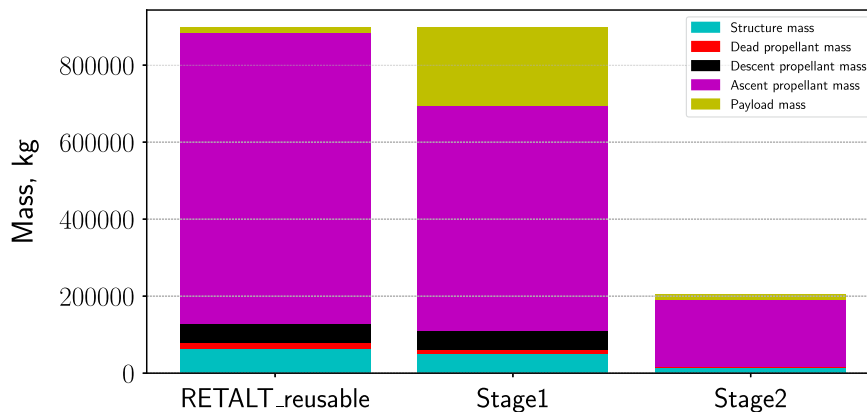
b) RETALT mass composition
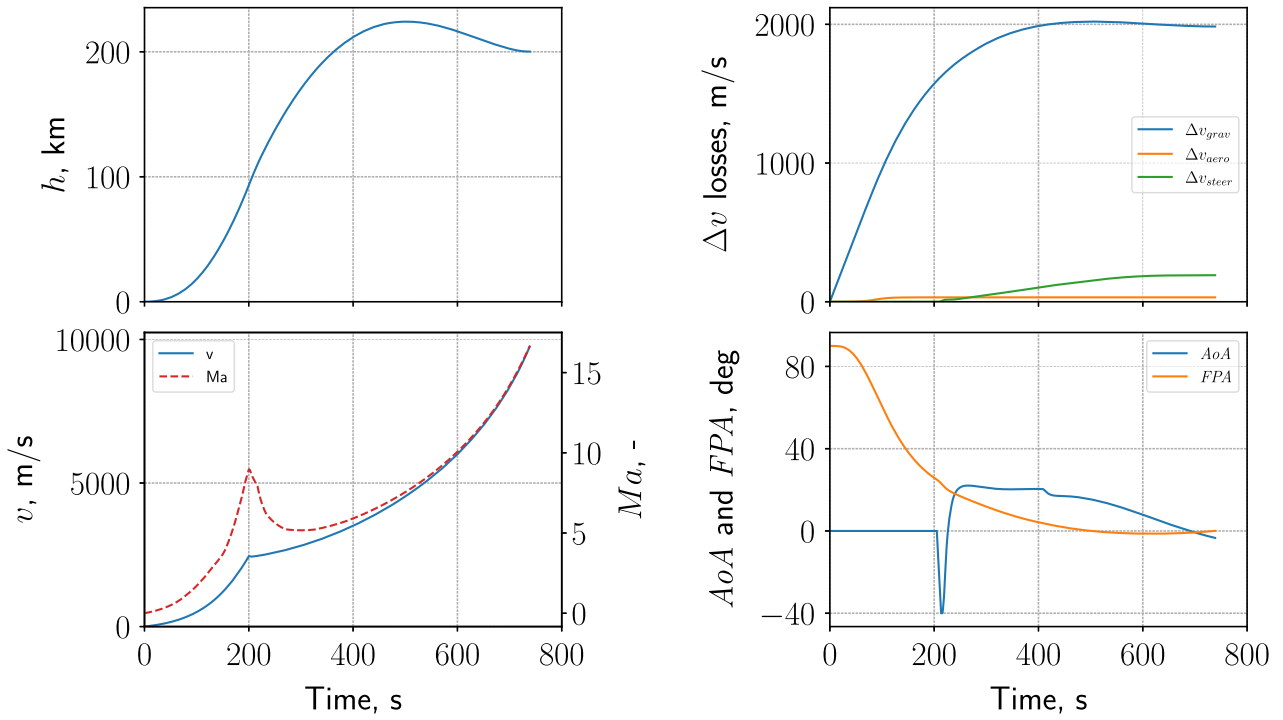
Fig. E1   Reusable launchers mass composition.
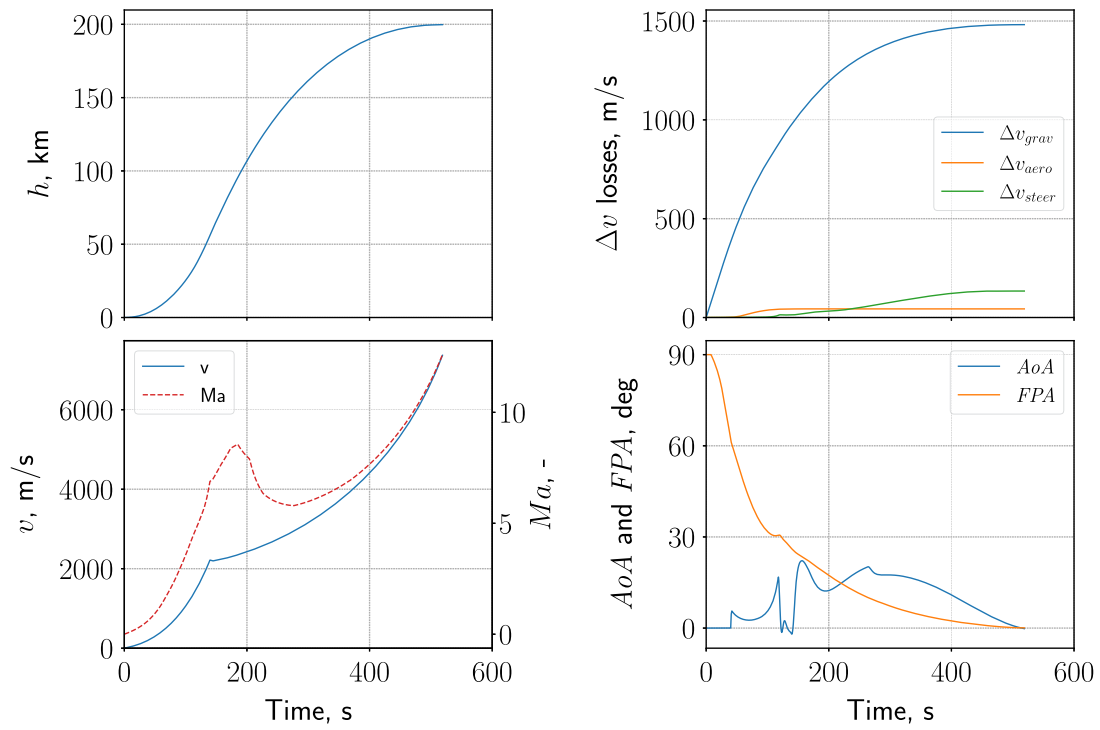
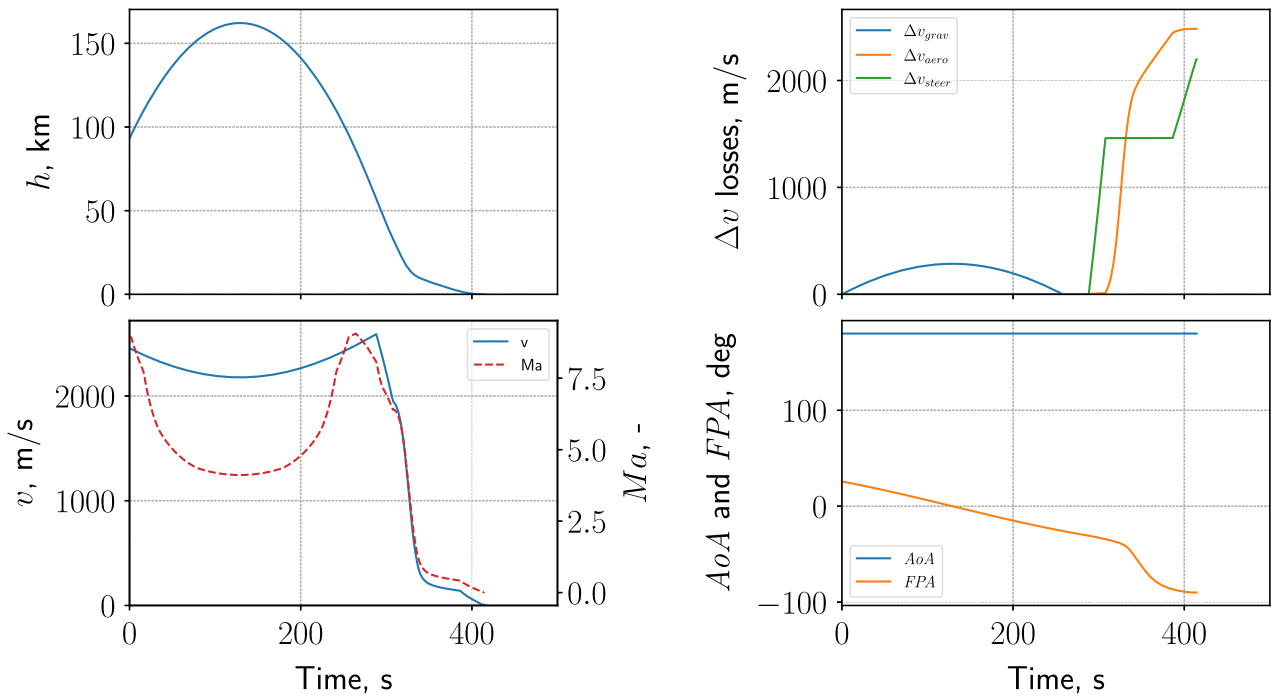a) **Ascent trajectory**

b) **Descent trajectory, max-q 120 kPa**

Fig. E2 Ascent and descent trajectories for the model of Falcon 9 FT.

a) Ascent trajectory

b) Descent trajectory, max-q 120 kPa

Fig. E3   Ascent and descent trajectories for the model of RETALT.
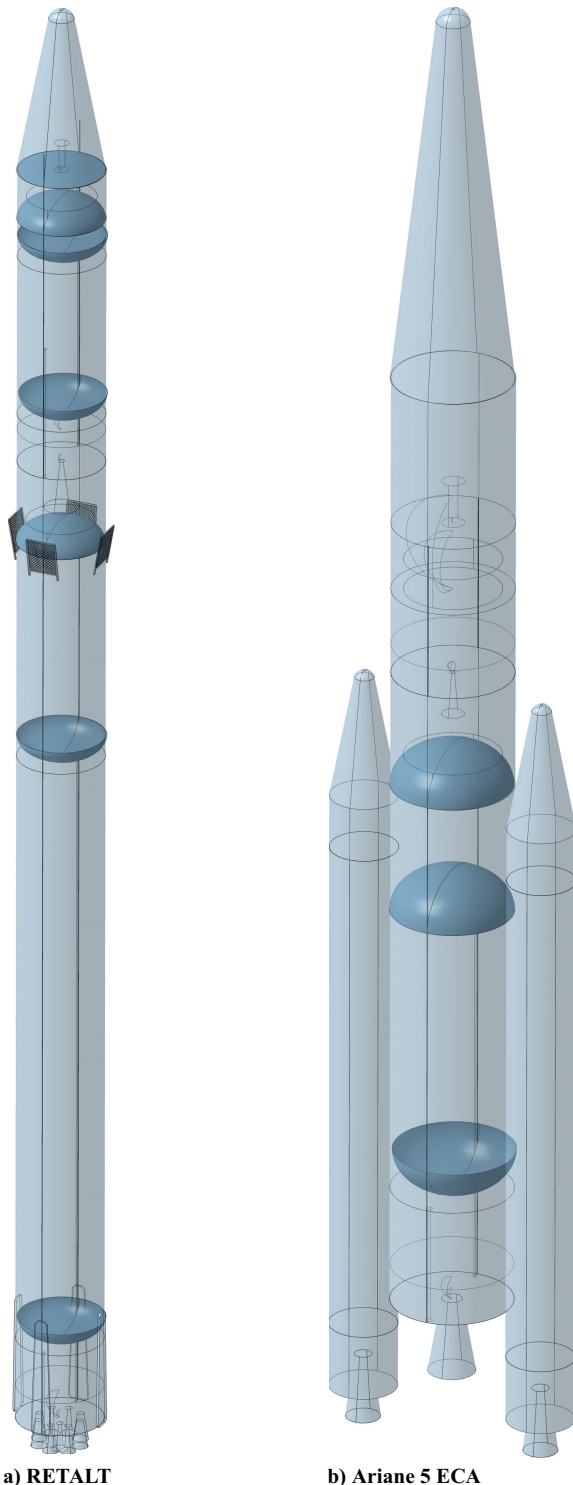
a) **RETALT**   b) **Ariane 5 ECA**

Fig. E4   Parametric CAD visualizations of RETALT and Ariane 5 ECA.

FT for ascent and descent are shown in Figs. E2 and E3. Examples of parametric visualizations of launchers are depicted in Fig. E4.

Acknowledgments

References

[1] Contant, S., "Design and Optimization of a Small Reusable Launch Vehicle Using Vertical Landing Techniques," Master's Thesis, Delft Univ. of Technology, Delft, The Netherlands, 2019.

[2] Jentzsch, S., "Optimization of a Reusable Launch Vehicle Using Genetic Algorithms," Master's Thesis, RWTH Aachen Univ., Inst. of Jet Propulsion and Turbomachinery, Aachen, Germany, 2020.

[3] Sippel, M., "Concurrent Launcher Engineering at DLR," *Concurrent Engineering Workshop (ESTEC)*, ESTEC, Noordwijk, 2004, https://www.dlr.de/Portaldata/55/Resources/dokumente/sart/ESAConcEng04.pdf.

[4] Wilken, J., and Stappert, S., "Comparative Analysis of European Vertical Landing Reusable First Stage Concepts," *CEAS Space Journal*, 2024.
https://doi.org/10.1007/s12567-024-00549-9

[5] Castellini, F., "Multidisciplinary Design Optimization for Expendable Launch Vehicles," Ph.D. Thesis, Politecnico di Milano, Aerospace Engineering Dept., Milano, Italy, 2012.

[6] Edberg, D., and Costa, W., *Design of Rockets and Space Launch Vehicles*, 2nd ed., AIAA, Reston, VA, 2022.
https://doi.org/10.2514/4.106422

[7] Goldyn, P., "Development of a Tool for Design of Reusable Space Transport Systems," Master's Thesis, RWTH Aachen, Institut für Luft- und Raumfahrttechnik, Aachen, Germany, 2023.

[8] Klevanski, J., and Sippel, M., "Beschreibung des Programms zur aerodynamischen Voranalyse CAC Version 2," Institut für Raumfahrtantriebe, Deutsches Zentrum für Luft- und Raumfahrt e.V, TR 647-2003/04, Lampoldshausen, Germany, 2003, https://elib.dlr.de/1623/.

[9] Hüniken, T., "Trajektoriensimulation für wiederverwendbare Trägersysteme mit komplexen aerodynamischen Datenbanken," Bachelor's Thesis, Technische Universität Braunschweig, Institut für Raumfahrtsysteme, Braunschweig, Germany, 2023.

[10] Curtis, H. D., *Orbital Mechanics for Engineering Students*, 1st ed., Elsevier Butterworth-Heinemann, 2005, pp. 560–579.

[11] Civek-Coşkun, E., and Özgören, K., "A Generalized Staging Optimization Program for Space Launch Vehicles," *6th International Conference on Recent Advances in Space Technologies (RAST)*, Istanbul, Turkey, 2013, pp. 857–862.
https://doi.org/10.1109/RAST.2013.6581333

[12] Marwege, A., Gülhan, A., Klevanski, J., Riehmer, J., Kirchheck, D., Karl, S., Bonetti, D., Vos, J., Jevons, M., Krammer, A., et al., "Retro Propulsion Assisted Landing Technologies (RETALT): Current Status and Outlook of the EU Funded Project on Reusable Launch Vehicles," *70th International Astronautical Congress (IAC)*, Washington, D.C., 2019, Paper IAC-19.D2.4.5x49370.

[13] Kirchheck, D., Marwege, A., Klevanski, J., Riehmer, J., Gülhan, A., Karl, S., and Gloth, O., "Validation of Wind Tunnel Test and CFD Techniques for Retro-Propulsion (RETPRO): Overview on a Project Within the Future Launchers Preparatory Programme (FLPP)," *International Conference on Flight Vehicles, Aerothermodynamics and Re-Entry Missions and Engineering (FAR)*, Monopoli, Italy, 2019.

[14] Dumont, E., Stappert, S., Ecker, T., Wilken, J., Karl, S., Krummen, S., and Sippel, M., "Evaluation of Future Ariane Reusable VTOL Booster Stages," *68th International Astronautical Congress (IAC)*, IAC Paper 17-D2.4.3, Adelaide, Australia, Sept. 2017.

[15] Sutton, G. P., and Biblarz, O., *Rocket Propulsion Elements*, 7th ed., Wiley, Hoboken, NJ, 2001, p. 107.

[16] Dergarabedian, P., and Dyke, R. T., "Estimating Performance Capabilities of Boost Rockets," Space Technology Lab. TR 59-0000-00792, Los Angeles, CA, 1959.

[17] Ambrosio, A., Burgess, P. D., Culver, H. D., Jensen, A. A., Werts, D. D., White, J. F., and Wine, B. A., "Flight Performance Handbook for Powered Flight Operations, Flight Mechanics and Space Vehicle Design, Empirical Formulae, Analytic Approximations and Graphical Aids," Space Technology Lab. TR 19620003901, Los Angeles, 1962.

[18] Marwege, A., Klevanski, J., and Riehmer, J., "System Definition Report: RETALT," Institut für Aerodynamik und Strömungstechnik, Abteilung für Über- und Hyperschalltechnologien Deutsches Zentrum für Luft- und Raumfahrt e.V TR, Köln-Porz, Germany, 2019.

[19] Deutsches Institut für Normung, *DIN 1319-4: Grundlagen der Meßtechnik, Teil 4: Auswertung von Messungen Meßunsicherheit*, Beuth Verlag, Berlin, 1999.

[20] Lobanovsky, Y. I., "Prediction of the Characteristic Velocity Calculation of Low-Earth Orbit Injection," 2023, https://synerjetics.ru/article/prediction.pdf [retrieved 24 Sept. 2023].

[21] Nikishchenko, I., "Launcher Calculator Source Code," 2023, https://launchercalculator.com [retrieved 24 Sept. 2023].

[22] *Space Data*, 5th ed., Northrop Grumman Space Technology, Dulles, VA, 2003.

[23] Klevanski, J., "Analyse der Stabilität und Steuerbarkeit von elastischen, mehrstufigen Raumtransportsystemen in der Vorentwurfsphase," Ph.D. Thesis, RWTH Aachen, Aachen, North Rhine-Westphalia, Germany, 2010.

[24] Falcon User's Guide, SpaceX, Sept. 2021, pp. 11–12, https://www.spacex.com/media/falcon-users-guide-2021-09.pdf.

[25] National Aeronautics and Space Administration, "Space Launch Report: SpaceX Falcon 9 v1.2 Data Sheet," TR XXXXX, 2018, https://sma.nasa.gov/LaunchVehicle/assets/spacex-falcon-9-v1.2-data-sheet.pdf.

[26] Wevolver, "Merlin Engine (Merlin-1D) - Falcon 9 and Falcon Heavy," 2023, https://www.wevolver.com/specs/merlin-engine-merlin-1d-falcon-9-falcon-heavy.

[27] Wevolver, "Falcon Heavy Block 5," 2023, https://www.wevolver.com/specs/falcon-heavy-block-5.

[28] *Ariane 5 User's Manual*, Arianespace, June 2020, https://www.arianespace.com/wp-content/uploads/2016/10/Ariane5-users-manual-Jun2020.pdf.

[29] National Aeronautics and Space Administration, "Space Launch Report: Ariane 5 Data Sheet, TR XXXXX, 2018, https://sma.nasa.gov/LaunchVehicle/assets/ariane-5-data-sheet.pdf.

[30] Centre national d'études spatiales, "Ariane 5 Technical Features," Nov. 2020, https://ariane5.cnes.fr/en/technical-features-0.

[31] Arianespace, "EAP—Solid Rocket Boosters," 2023, https://www.arianespace.com/?popup=ariane-5-6.

[32] SpaceX, "Capabilities and Services," 2023, https://www.spacex.com/media/Capabilities&Services.pdf.

[33] Weiland, C., *Computational Space Flight Mechanics*, 1st ed., Springer-Verlag, Berlin, 2010, p. 141, https://books.google.de/books?id=ouIUPqnqXZAC.

[34] Akin, D. L., "Mass Estimating Relations," Lecture Notes, Course ENAE 483/788D—Principles of Space Systems Design, Univ. of Maryland, College Park, MD, 2022.

[35] Brown, C., *Elements of Spacecraft Design*, 1st ed., AIAA, Reston, VA, 2002, p. 27.

[36] Rohrschneider, R. R., "Development of a Mass Estimating Relationship Database for Launch Vehicle Conceptual Design," Tech Rept., Georgia Inst. of Technology, 2002.

[37] Kreis, O., "Stufungsoptimierung für Ein Trägersystem Mit LOX/MethanAntrieb, DLR-LA-RAS-RP-010," Institut für Raumfahrtantriebe, Deutsches Zentrum für Luft- und Raumfahrt e.V, TR DLR-LA-RAS-RP-010, Lampoldshausen, Germany, 2014.

[38] Kirchheck, D., and Klevanski, J., "Reference Case Definition File: RETPRO: Validation of Wind Tunnel Test and CFD Techniques for Retro-Propulsion. FLPP-RETPRO-DLR-2019-RP-001, Institut für Aerodynamik und Strömungstechnik, Abteilung für Über- und Hyperschalltechnologien, Deutsches Zentrum für Luft- und Raumfahrt e.V, TR FLPP-RETPRO-DLR-2019-RP-001, Köln-Porz, Germany, 2023.

C. Bonnal
Associate Editor